

**SUPERCURRENTS AND PERSISTENT CURRENTS IN  
STRONGLY CORRELATED ELECTRON SYSTEMS**

**A THESIS  
SUBMITTED TO THE DEPARTMENT OF PHYSICS  
AND THE INSTITUTE OF ENGINEERING AND SCIENCE  
OF BILKENT UNIVERSITY  
IN PARTIAL FULFILLMENT OF THE REQUIREMENTS  
FOR THE DEGREE OF  
MASTER OF SCIENCE**

**By  
Hüseyin Boyacı  
September 1995**

QC  
176.8  
.E4  
369  
1995

SUPERCURRENTS AND PERSISTENT CURRENTS IN  
STRONGLY CORRELATED ELECTRON SYSTEMS

A THESIS

SUBMITTED TO THE DEPARTMENT OF PHYSICS  
AND THE INSTITUTE OF ENGINEERING AND SCIENCE  
OF BILKENT UNIVERSITY  
IN PARTIAL FULFILLMENT OF THE REQUIREMENTS  
FOR THE DEGREE OF  
MASTER OF SCIENCE

By

Hüseyin Boyacı

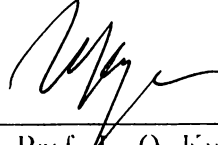
September 1995

Hüseyin Boyacı  
*Hüseyin Boyacı*

QC  
176.8  
.E4  
B69  
1995

BC31886

I certify that I have read this thesis and that in my opinion it is fully adequate, in scope and in quality, as a dissertation for the degree of Master of Science.



---

Prof. T. O. Kulik (Supervisor)

I certify that I have read this thesis and that in my opinion it is fully adequate, in scope and in quality, as a dissertation for the degree of Master of Science.



---

Prof. A. S. Shumovsky

I certify that I have read this thesis and that in my opinion it is fully adequate, in scope and in quality, as a dissertation for the degree of Master of Science.



---

Asst. Prof. Ekimel Özbay

Approved for the Institute of Engineering and Science:



---

Prof. Mehmet Baray  
Director of Institute of Engineering and Science

# Abstract

## SUPERCURRENTS AND PERSISTENT CURRENTS IN STRONGLY CORRELATED ELECTRON SYSTEMS

Hüseyin Boyacı

M. S. in Physics

Supervisor: Prof. I. O. Kulik

September 1995

The full understanding of the solution for the 1-d Hubbard model is of interest in its own right, and may provide clues to the understanding of higher dimensional systems. We have found the exact solution of the model for two electrons, with a magnetic flux applied, and showed some new results. We have also made calculations for more than two electrons on a loop with a magnetic flux through it, using the Bethe-ansatz equations. Within the assumption that oxygen orbitals may play a fundamental role in the superconductive properties of  $Cu - O$  high  $T_c$  materials, exact calculations of the ground-state energy for two electrons in the contraction mechanism have been performed. To test the beginning assumption, some numerical calculations have been presented.

**Keywords:** strongly correlated electron systems, 1-d Hubbard model, contraction model, high  $T_c$  superconductivity, mesoscopics.

# Özet

## KUVVETLİ ETKİLEŞEN ELEKTRON SİSTEMLERİNDE ÜSTÜN AKIM VE KALICI AKIM

Hüseyin Boyacı

Fizik Yüksek Lisans

Tez Yöneticisi: Prof. I . O. Kulik

Eylül 1995

1-b Hubbard modelinin çözümünün tam olarak anlaşılması kendi başına ilgi çekicidir ve daha yüksek boyutlu sistemlerin anlaşılması için ipuçları sağlayabilir. Modelin, bir manyetik akı uygulanarak iki elektron için kesin çözümlerini bulduk ve bazı yeni sonuçlar gösterdik. Ayrıca, içinden manyetik akı geçen bir halkada, iki elektrondan fazlası için Bethe-ansatz denklemlerini kullanarak hesaplamalar yaptık. Oksijen yörüngelerinin  $Cu - O$  yüksek  $T_c$  malzemelerinin süperiletkenlik özelliklerinde temel bir rol oynayabileceği varsayımıyla, iki elektron için büzülme mekanizmasında temel-durum enerjisinin kesin hesaplamaları yapıldı. Başlangıç varsayımını test etmek için bazı sayısal hesaplamalar gösterildi.

### Anahtar

**sözcükler:** kuvvetli etkileşen elektron sistemleri, 1-b Hubbard modeli, büzülme modeli, yüksek  $T_c$  süperiletkenliği, mezoskopik.

# Acknowledgement

It is my pleasure to express my deepest gratitude to Prof. I. O. Kulik for his supervision to my graduate study. Without his excellent logic and knowledge non of this work could have been produced.

I wish to express my thanks to the faculty and research assistants of Department of Physics in Bilkent University, especially to my residence-mates Özgür Özer and Hakan Türeci for their endurance toward any trouble that I caused in the course of our close interactions.

I appreciate moral support by many friends and everybody that I see in the building of Faculty of Science, everyday and every night, from the auxiliary staff and security members to the Dean of the Faculty and his secretary.

Very special thanks are due to İhsan Ecemiş, his sister Zeynep, and Erkan Tekman for many enjoying times and trips to lots of different places we had together, which gave me further encouragement and moral during my work.

Finally, my ultimate thanks are due to my family for their extreme interest and support.

# Contents

Abstract	i
Özet	ii
Acknowledgement	iii
Contents	iv
List of Figures	vi
<b>1 INTRODUCTION</b>	<b>1</b>
1.1 Aharanov-Bohm Effect . . . . .	3
1.2 Persistent Currents in Mesoscopic Structures . . . . .	10
1.3 Strongly Correlated Models of High- $T_c$ Superconductivity . . . . .	15
<b>2 1-D HUBBARD MODEL</b>	<b>26</b>
2.1 Ground State Energy of Two Electrons . . . . .	28
2.1.1 The Dependence of Amplitude of Energy Oscillations on the Number of Sites . . . . .	36
2.2 Discrete Bethe-Ansatz Equations	40
2.2.1 $N_e = 2$ ( $\uparrow\downarrow$ ) . . . . .	43
2.2.2 $N_e = 4$ ( $\uparrow\uparrow\downarrow\downarrow$ ) . . . . .	45
2.2.3 $N_e = 6, 8, 10, \dots$ . . . . .	46

<b>3</b>	<b>CONTRACTION MODEL</b>	<b>49</b>
3.1	Bound States of Two Electrons	50
3.2	The Overlap Integral . . . . .	56
3.2.1	Interpretation of the Results . . . . .	59
<b>4</b>	<b>CONCLUSION</b>	<b>61</b>

# List of Figures

1.1	Magnetic AB effect. . . . .	5
1.2	AB effect on a single electron . . . . .	8
1.3	An exactly solvable example of AB effect. . . . .	9
1.4	Experiment carried out to observe the persistent current	12
1.5	Normal state quantum interferometer. . . . .	13
1.6	The effect of the impurities on the energy in the extended zone scheme. . . . .	15
1.7	Crystal structure of $La_2CuO_{4-y}$ . . . . .	17
1.8	Phase diagram of $La_{2-x}Sr_xCuO_{4-y}$ . . . . .	17
1.9	Structure of $RBa_2Cu_3O_7$ . . . . .	18
1.10	Phase diagram of $YBa_2Cu_3O_{7-\delta}$ . . . . .	19
1.11	Copper d-orbitals. . . . .	20
2.1	Sample configuration . . . . .	27
2.2	Plot of transcendental equation for 1-d Hubbard model with 2 electrons. . . . .	30
2.3	The poles of the integral in the complex plane. . . . .	31
2.4	Plot of the transcendental equation for $U > 0$ . . . . .	32
2.5	The plot of the transcendental equation for $U < 0$	33
2.6	Energy versus flux for two electrons. . . . .	35
2.7	The energy oscillations for 2 electrons. . . . .	37
2.8	The energy oscillations for $U > 0$ for $N_a = 50$ . . . . .	37
2.9	The amplitude of oscillations for $U < 0$ with $N_a = 50$ . . . . .	38
2.10	The current $J(\Phi)$ for two electrons. . . . .	39

2.11	The dependence of energy on the flux for $N_r = 4$ . . . . .	47
3.1	Intrinsic-electron and intrinsic-hole type metals. . . . .	50
3.2	Plot of the transcendental equation for the contraction model . .	54
3.3	Energy versus flux for two electrons in the contraction mechanism.	55
3.4	The $CuO_2$ network. . . . .	57
3.5	Overlapping orbitals of the oxygen atoms. . . . .	58
3.6	Energy versus flux with the results of overlap integration. . . . .	59

# Chapter 1

## INTRODUCTION

Much of solid state theory and statistical physics is concerned with the properties of macroscopic systems. These are often calculated using the ‘thermodynamic limit’ (system’s volume  $\Omega$ , and particle number  $N$ , tending to infinity with  $n \sim N/\Omega$  constant) which is a convenient mathematical device for obtaining bulk properties. Usually, the system approaches the macroscopic limit once its size is much larger than some correlation length,  $\xi$ . In most cases  $\xi$  is of the order of a microscopic length (e.g.,  $\sim n^{-1/3}$ ), but in some special cases, such as in the vicinity of a second-order transition,  $\xi$  can become very large and one may observe behavior which is different from the macroscopic limit for a large range of sample sizes.<sup>1,2</sup> The effective length scale dividing microscopic from macroscopic behavior becomes very large when the conducting (or semiconducting) systems are small and at low temperatures. Here, once an electron can propagate across the whole system without inelastic scattering, its wave function will maintain a definite phase and it will, thus, be able to exhibit a variety of novel interesting interference phenomena.

The interest in studying these systems in the intermediate size range between microscopic and macroscopic- sometimes referred to as the ‘mesoscopic’ (a word coined by Van Kampen, 1976, as derived from the Greek prefix meso  $\equiv$  middle) range- is not only for understanding the macroscopic limit, and how it is achieved by, say, building up larger and larger clusters to go from a ‘molecule’

to the ‘bulk’. The term mesoscopic corresponds to a length scale for which the averaging properties of the macroscopic world does not take place, and the reversible and perfect mechanics of microscopic objects are applicable.<sup>5,6,8,61</sup>

Formal definition of mesoscopic object is that the phase scattering length of electron should be larger than the size of specimen,  $d$ . Elastic scattering length may be much smaller (diffusive mesoscopic regime) or larger (ballistic mesoscopic regime) than  $d$ .

Formally mesoscopic objects are those not possessing the property of self-averaging, that is, independent from specific microscopic parameters of their properties, which are defined by average quantities like impurity concentration. However, small systems with  $d$  less than, say,  $1\mu m$  are often considered as ‘mesoscopic’.

The special phenomena that exists in this range are of great interest in themselves. Another interesting aspect is the distinction<sup>11,15,16,13</sup> between ensemble-averaged properties and those specific to a particular given small system prepared under the same macroscopic constraints as with all the ensemble members. The specific ‘fingerprint’ of such a small system is of interest and may be used to obtain some statistical information on the particular arrangement of the constituents in the system.<sup>15</sup> Many of the usual rules that one is used to in macroscopic physics may not hold in ‘mesoscopic’ systems. For example the rules for addition of resistances, both in series<sup>11,16</sup> and in parallel<sup>17,18</sup> are different and more complicated. The electron motion is wave-like and is similar to that of electromagnetic radiation in waveguide structures, except for complications due to disorder. These effects may set fundamental limits on how small various electronic devices can go. On the other hand, ideas for new devices, such as those operating in analogy<sup>12,20</sup> with various optical and waveguide ones, as well as with SQUIDs (Superconducting Quantum Interference Devices), and other Josephson-effect systems,<sup>43</sup> may emerge for small normal conductors.

The technology<sup>12</sup> for the fabrication of structures with very small sizes, using advanced optical or x-ray lithographic techniques, as well as electron-beam, is advancing very quickly, and has reached the stage where many theoretical

predictions can now be confronted by experimental results.

To achieve higher operation speeds and less power consumption, one of the most important objectives of the electronics technology became miniaturizing of the devices. Yet, small can not be beautiful unless the device operates according to the expectations. There are physical limitations in addition to the technological ones opposing the miniaturization trend. After all, a smaller ohmic contact has to be an ohmic contact with smaller conductance and so on.

One of the most important features of the small systems is their sample specific properties. For small systems the rule due to our '*macroscopic*' everyday experience, telling macroscopically identical systems have to yield the same results under identical experimental conditions breaks down. As an example, ohmic contacts fabricated on the same wafer using the same chemical and physical modification steps may have widely spread resistance values. For a large contact, there is a large number of grains (the metal-semiconductor contact is not ordered and is made of grains) and the measured resistance is essentially an average of resistance of these grains. While, a small contact has only a small number of grains and this averaging can not be complete.

Another important aspect of small systems is the geometry-specific properties. Miniaturizing the devices further, one reaches to a limit for which the device does not contain any impurities at all. For this case, the material properties are suppressed for a large extent, while quantum mechanical propagation along the sample becomes essential.

For further reading, see the reference by I. O. Kulik<sup>47</sup> and the references therein.

## 1.1 Aharanov-Bohm Effect

According to standard quantum mechanics, the motion of a charged particle can sometimes be influenced by electromagnetic fields in regions from which the particle is rigorously excluded.<sup>23,24</sup> This phenomenon has come to be called the Aharanov-Bohm effect (AB effect), after the seminal 1959 paper entitled

‘Significance of Electromagnetic Potentials in the Quantum Theory’, by Y. Aharonov and D. Bohm.<sup>24</sup> What AB effect teaches us about the significance of the electromagnetic potentials has since been discussed from several points of view,<sup>26,29,25,28,7,58</sup> on the assumption that standard quantum is indeed a correct description of nature.

The experimental quantization of the fluxoid in superconducting rings and in Josephson junctions has been interpreted as an experimental confirmation of AB effect.<sup>53</sup> Interference experiments on electron beams have been carried out to provide more direct information, with increasing precision and especially with increasing control of stray fields that might obscure the implications of the experiments.<sup>30,27,57</sup>

In the magnetic version of the AB effect, a stationary magnetic field is introduced in the region between the two beams, as in Figure 1.1. The electrons are forever rigorously excluded from that region by some baffles. Similarly, magnetic flux is made to avoid the regions where the electrons are permitted. The Hamiltonian  $H$  and the time independent wave function  $\psi(\mathbf{x})$  are given by

$$H = \frac{1}{2m} \left[ -i\hbar\nabla + \frac{e}{c}\mathbf{A}_e \right]^2 - eV_0(\mathbf{x}) \quad (1.1)$$

$$\psi(\mathbf{x}) = \psi_0(\mathbf{x}) \exp \left\{ \frac{-iS(\mathbf{x})}{\hbar} \right\} \quad (1.2)$$

where  $A_e(\mathbf{x})$  is the vector potential due to the excluded magnetic field and  $S(\mathbf{x})$  is the line integral

$$S(\mathbf{x}) = -\frac{e}{c} \int^{\mathbf{x}} \mathbf{A}_e(\mathbf{x}') \cdot d\mathbf{x}' \quad (1.3)$$

and the path of integration is taken along the arm of the interferometer containing the point  $\mathbf{x}$ .  $\psi_0(\mathbf{x})$  is the wave function in the absence of the excluded magnetic field presented by  $\mathbf{A}_e(\mathbf{x})$ , and  $V_0$  represents possible electrostatic potentials to steer the beam which do not depend upon the excluded magnetic field.

If the magnetic flux  $\Phi$  through the coil is nonvanishing, the vector potential  $A_e(\mathbf{x})$  cannot vanish everywhere in the support of  $\psi_0(\mathbf{x})$ , because  $\oint \mathbf{A}_e(\mathbf{x}) \cdot d\mathbf{x}$  on a closed path drawn around the coil through the two arms of the interferometer is equal to  $\Phi$ .

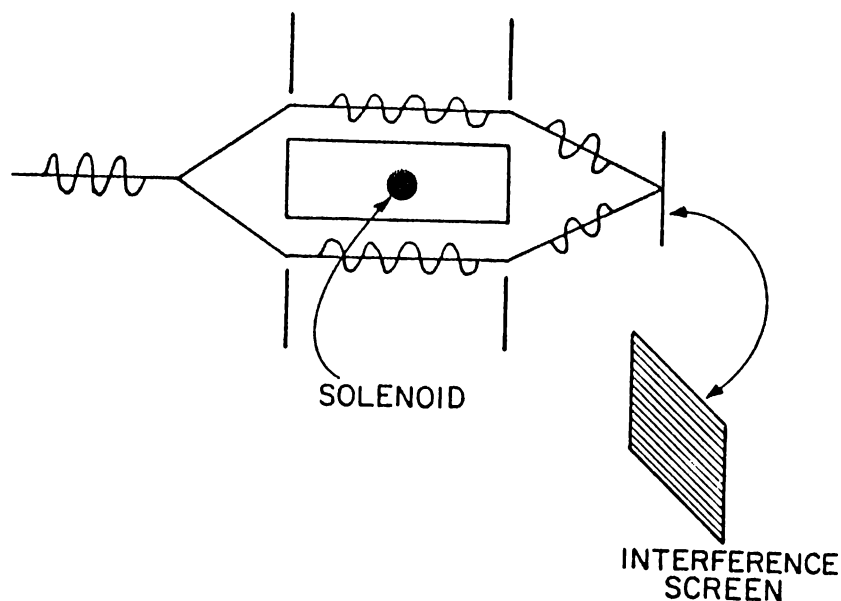


**Figure 1.1:** Magnetic AB effect.

The axis of the solenoid  $\Phi$  is perpendicular to the page. The wave function is a split plane wave.

In the interference region, the phase shift between the two beams is

$$\Delta\phi = \frac{S_2 - S_1}{\hbar} = \frac{e}{\hbar c} \Phi \quad (1.4)$$

where  $S_2$  and  $S_1$  are the action integrals of Eq. (1.3), calculated along the upper and lower arms of the interferometer.

The phase shift  $\Delta\phi$  between the beams in the two arms of the interferometer is gauge invariant, as it must be, depending only upon the magnetic flux through the excluded region. The interference pattern is therefore a periodic function of that magnetic flux, with period equal to London's unit, a flux quantum

$$\Phi_0 = \frac{2\pi\hbar c}{e} = \frac{hc}{e} \quad (1.5)$$

However, there is no Aharonov-Bohm effect in classical physics. AB effect enters quantum mechanics through the appearance of electromagnetic potentials  $V_e$  and  $\mathbf{A}_e$  in the Hamiltonian and consequently in the Schrödinger equation. The local Maxwell fields  $\mathbf{E}$  and  $\mathbf{B}$  appears only in the discussion, never in the equations of motion.

When classical theory is presented in the Lagrangian or Hamiltonian formulation, the potentials appear just as they do in quantum theory. However, we know that those formulations of classical physics are equivalent to Newton's laws, so the motion of a charged particle is completely determined by the local electric and magnetic fields acting upon it. Newton's second law and the Lorentz force equation give

$$m \frac{d^2 \mathbf{r}}{dt^2} = -e \left[ \mathbf{E} + \frac{\mathbf{v}}{c} \times \mathbf{B} \right] \quad (1.6)$$

and nothing more is needed. To remove this feature of the classical theory in the case of a multiply connected region is not a promising enterprise because the local conservation of energy and momentum between the particles and fields depends upon it. Therefore, it is no surprise that the AB effect depends upon flux or the action in units proportional to Planck's constant  $\hbar$ , which is peculiar to quantum theory. Attempts have nevertheless been made to obtain AB effect from classical or semiclassical theory.<sup>54</sup>

Quantum theory unavoidably relies upon the Hamiltonian or Lagrangian formulation of the dynamics, where the local electromagnetic fields disappear from the equations of motion in favor of the scalar and vector potentials. The classical argument that the equations of motion are equivalent to Newton's second law with the local  $\mathbf{E}$  and  $\mathbf{B}$  fields does not apply to quantum mechanics, and remote fields may have observable effects in some cases. For instance, if a magnetic field  $\mathbf{B}_e(\mathbf{x})$  is confined to the interior of a torus from which electron is excluded,<sup>32</sup> the vector potential  $\mathbf{A}_e(\mathbf{x})$  cannot vanish throughout the region outside the torus, and it appears in the Schrödinger equation. The vector potential can not be removed from the domain of the electron by a gauge transformation because

$$\int \mathbf{A}_e(\mathbf{x}) \cdot d\mathbf{x} = \Phi_e \quad (1.7)$$

where the path of integration links the torus and  $\Phi_e$  is the magnetic flux through the torus.

In the absence of the excluded magnetic field,

$$i\hbar \left( \frac{\partial \psi_0}{\partial t} \right) = H_0 \psi_0(\mathbf{x}, t) = \frac{1}{2m} \left[ -i\hbar \nabla + \frac{e}{c} \mathbf{A}_0(\mathbf{x}, t) \right]^2 \psi_0 - eV_0(\mathbf{x}, t) \psi_0 \quad (1.8)$$

where  $V_0(\mathbf{x}, t)$  and  $\mathbf{A}_0(\mathbf{x}, t)$  are the potentials due to ordinary electromagnetic fields that may exist within the domain of the electron. With the addition of an excluded stationary magnetic field whose vector potential is  $\mathbf{A}_e(\mathbf{x})$

$$ih \left( \frac{\partial \psi}{\partial t} \right) = H \psi(\mathbf{x}, t) = \frac{1}{2m} \left[ -ih\nabla + \frac{e}{c} (\mathbf{A}_0(\mathbf{x}, t) + \mathbf{A}_e(\mathbf{x})) \right]^2 \psi - eV_0(\mathbf{x}, t)\psi \quad (1.9)$$

Formally,  $H$  and  $H_0$  are related by the gauge transformation

$$U(\mathbf{x}) = \exp \left\{ - \left( \frac{ic}{hc} \right) \int^{\mathbf{x}} \mathbf{A}_e(\mathbf{x}') \cdot d\mathbf{x}' \right\} \quad (1.10)$$

$$\psi = U\psi_0 \quad (1.11)$$

$$H = UH_0U^{-1} \quad (1.12)$$

It follows that  $H$  and  $H_0$  describe the same physics and the excluded magnetic field  $\mathbf{B}_e(\mathbf{x})$  has no observable influence on the dynamics of the electron, if Eqs. (1.10)-(1.12) apply.

However, for Eqs. (1.10)-(1.12) to be meaningful and  $\psi = U\psi_0$  to be a single valued solution of the Schrödinger equation (1.9),  $U$  must be a single valued function of  $\mathbf{x}$ , independent of the path of integration in the exponent in Eq. (1.10). When the domain of  $x$  is simply connected, it is sufficient for  $\mathbf{B}_e(x) = \nabla \times \mathbf{A}_e(\mathbf{x})$  to vanish everywhere within it. Then  $\int^{\mathbf{x}} \mathbf{A}_e(\mathbf{x}') \cdot d\mathbf{x}'$  is independent of the path of integration,  $U(\mathbf{x})$  is single valued, and there can be no observable effect of the excluded magnetic field. But when the domain of the electron is multiply connected as in Figure 1.2, and the magnetic field is confined to a region whose topology is that of an excluded cylinder or torus, Eq. (1.10) shows that  $U(\mathbf{x})$  may not be single valued even if  $\mathbf{B}_e(\mathbf{x})$  vanishes everywhere in the domain of the electron. Then there is no gauge transformation to connect  $H_0$  with  $H$ , and an observable AB effect is possible; the motion of the electron may depend upon the magnetic flux  $\Phi_e$  through the hole in the electron's domain.

There is an exceptional case. Because only  $U$  has to be single valued, not  $\int \mathbf{A}_e(\mathbf{x}) \cdot d\mathbf{x}$ , the AB effect disappears when the excluded flux  $\Phi_e = \oint \mathbf{A}_e(\mathbf{x}) \cdot d\mathbf{x}$  is an integer multiple of  $\Phi_0$ , i.e. when

$$\Phi_e = n \left( \frac{2\pi hc}{c} \right) \quad (1.13)$$

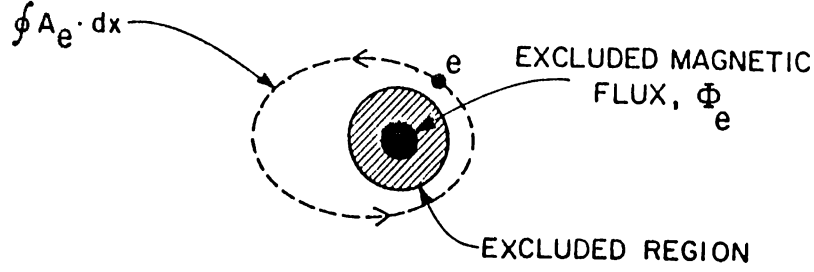


**Figure 1.2:** AB effect on a single electron

In that case integrating around the excluded flux changes  $U$  by the factor  $\exp(2\pi i)$ , and it remains single valued.

More generally, all observable phenomena depend only upon the flux  $\Phi_e$ , through the excluded region, and have period  $\Phi_0$ .

The simplest exactly solvable example of AB effect exhibits all the general features of the bound state problem. Consider an electron constrained to move on the circumference of a circle of radius  $r$  in the  $xy$  plane, as in Figure 1.3. An external magnetic flux  $\Phi$  goes up the  $z$  axis and returns uniformly along the surface of a cylinder whose radius is greater than  $r$ , so that there is no magnetic field at radius  $r$  where the electron moves.

In the gauge where  $\nabla \cdot \mathbf{A}$  vanishes,

$$\begin{aligned} A_\theta &= \frac{\Phi}{2\pi r} \\ A_\rho &= A_z = 0 \end{aligned} \quad (1.14)$$

The Hamiltonian for an electron of mass  $m$  is

$$H = \frac{1}{2mr^2} \left[ L_z + r \frac{e}{c} A_\theta \right]^2 = \frac{1}{2mr^2} \left[ L_z + \frac{e\Phi}{2\pi c} \right]^2 \quad (1.15)$$

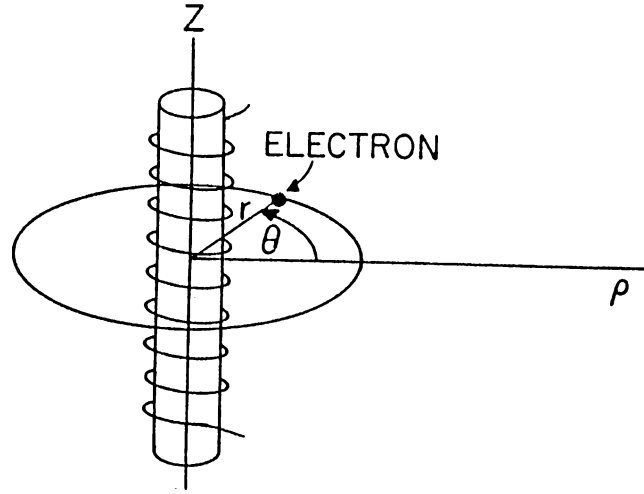


**Figure 1.3:** An exactly solvable example of AB effect.

The bound state wave functions and energies are

$$\psi_\ell(\theta) = \frac{1}{\sqrt{2\pi}} \exp(i\ell\theta) \quad (1.16)$$

$$E_\ell = \frac{1}{2mr^2} \left[ \ell h + \frac{c\Phi}{2\pi c} \right]^2 = \frac{h^2}{2mr^2} \left[ \ell + \frac{\Phi}{\Phi_0} \right]^2 \quad (1.17)$$

where  $\ell$  are integers. The state  $\psi_\ell$  has definite canonical angular momentum  $L_z$  and kinetic angular momentum  $K_z$ , given by

$$L_z = \ell h \quad (1.18)$$

$$K_z = mr^2\dot{\theta} = \left( L_z + \frac{c\Phi}{2\pi c} \right) = h \left( \ell + \frac{\Phi}{\Phi_0} \right) \quad (1.19)$$

and the Hamiltonian is equal to the  $K_z^2/2mr^2$ .

Equations (1.17) and (1.19) clearly display the flux dependence of the energy spectrum and kinetic angular momentum, both measurable quantities in principle. Both spectra are periodic in  $\Phi$  with period  $\Phi_0$ , as expected.

The first experiments using solid state devices were carried out by Sharvin and Sharvin<sup>56</sup> and Al'tshuler and coworkers.<sup>33</sup> It took a few years for the western experimentalists to reproduce these results. Strikingly the period of oscillations

was found to be  $\Phi_0/2$ , and not  $\Phi_0$  as expected. This point was clarified by Al'tshuler and coworkers.<sup>33,34</sup> According to their explanation, the  $\Phi_0/2$  oscillation arise due to the interference of electrons enclosing the cylinder once clockwise and counterclockwise. Then the phase difference is twice of the expected value and thus, the period halves.

In a pure ring, the electron wave turns over the ring just one time ( $hc/e$  oscillations-non-self-averaging effect changing sign of current in the ring from sample to sample), but in a dirty ring two electron waves with clockwise and counterclockwise revolutions both contribute to flux-dependent conduction ( $hc/2e$  oscillations- self-averaging; weak localization effect not changing sign from sample to sample.) ( $\Delta\Phi = 2\pi\Phi/\Phi_0$  and  $4\pi\Phi/\Phi_0$  respectively).

In the interesting paper of T. H. Boyer<sup>37</sup> it is pointed out that accounts in the literature sometimes misinterpreted the Aharonov-Bohm effect. For additional reading, one can refer to the book by Peshkin and Tonomura.<sup>54</sup>

## 1.2 Persistent Currents in Mesoscopic Structures

When someone talks about a non-decaying or 'persistent' current, the question 'how can a current in an isolated metallic ring flow infinitely?' arises immediately. Our common experience tells us that any non-decaying current needs a driving force to supply the necessary energy to compensate the losses due to the transfer of energy ('Joule heating') from moving electrons to atomic vibrations (phonons) and other elementary excitations in the solid. If the metal is superconducting and the temperature and magnetic field are below the critical values, these losses vanish. However, in a normal, nonsuperconducting metal loop a persistent current can also flow without dissipation for infinitely long time. For such a flow of current, it is required that the metal loop be small enough and temperature be low enough to enter into the domain of quantum physics.

At low enough temperatures, a small metallic loop behaves similar to an atom

or a molecule like benzol molecule. Although the atom in question is quite large (approximately 1 micrometer in diameter which is more than  $10^3$  times of the size of normal atoms), but still small for the standards of everyday life.

The possibility of persistent current in a loop arises due to Aharonov-Bohm effect, which is a peculiar property of quantum mechanical world. As we explicitly showed in the previous section, the wave function of an electron senses the magnetic field well away from the electron (this is called nonlocality). The vector potential rather than the magnetic field itself enters the equations of the quantum mechanics and changes the phase of the electron wave function in such away that the electron energy becomes a periodic function of flux with a period  $\Phi_0 = hc/e$ , which is called ‘flux quantum’. Although the quantum is quite small ( $\Phi_0 = 4.10^{-13}T.m^2$ ) since it is proportional to Planck constant  $h$ , it changes electron energy drastically. Therefore the laws of electromagnetism suggest that a current should appear which is the derivative of energy with respect to flux- $\Phi$ . Unlike the conventional Ohmic current in metals or semiconductors, this current is absolutely stable and can flow at zero voltage without dissipation. At a given  $\Phi$ , persistent current minimizes the loop energy irrelevant to whether the magnetic field is zero or nonzero at the place where electrons are. In particular we can place our ring in an external homogeneous magnetic field and get the value of the persistent current appropriate to the amount of flux enclosed by the ring.

In a pure metallic sample of finite size, current arises as a consequence of the dependence of the energy on the vector potential  $A$  in a ring. This current is equal to

$$j = \frac{e\hbar}{m} \left( K_n - \frac{eA}{hc} \right) \quad (1.20)$$

where  $K_n = (2\pi/L)n$ .

In large system,  $K$  changes in such a way that ‘paramagnetic’ contribution to the current,  $e\hbar K/m$ , compensates for the ‘diamagnetic’ term,  $-(e^2/mc)A$ . However, in small system,  $K$  is quantized and therefore  $j$  cannot be zero. This property remains even if both elastic and inelastic scattering is introduced.

The theoretical prediction of the effect goes back to 1970 when the phenomenon was substantiated in the Kharkov Physico-Technical Institute.<sup>22</sup>

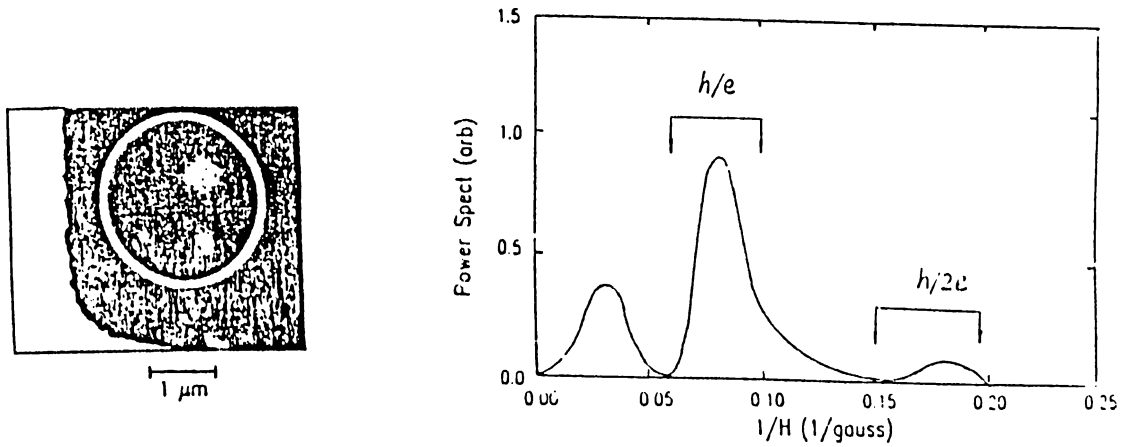


**Figure 1.4:** Experiment carried out to observe the persistent current. Actually the current itself is not observed, rather the magnetic moment of the tiny golden loop produced by the persistent current was observed.

Later, the effect was rediscovered by IBM scientists in 1983, again theoretically,<sup>38</sup> but it took almost next 10 years to actually observe this phenomenon which was accomplished in the IBM Laboratory.<sup>39</sup> What was observed was not a current itself but a magnetic moment of a tiny golden loop produced by a persistent current in the loop, oscillating as a function of magnetic field with the period  $\Phi_0/S$ , where  $S$  is the cross section of the loop.

The effect may look as purely academic at present. Nevertheless, it promises some new possibilities to the up-to-date microelectronics. This is a new kind of nonlinearity, the property which is necessary for the operation of any computer of electronic sensor. And extremely fast one! The other possibility is the measurement of the magnetic field in a very large range from very small to extremely large values, by just counting the flux quanta. This can be accomplished more easily by measuring the transverse resistance of a loop vs flux (Figure 1.5). Resistance change is due to a persistent current, which in the upper branch adds to and in the lower branch extracts from an Ohmic current, and due to the nonlinearity of the interaction between both currents. The device of Figure

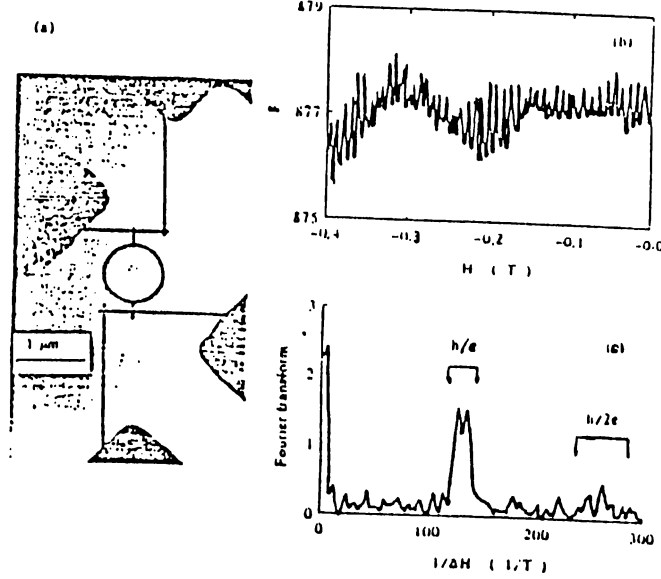


**Figure 1.5:** Normal state quantum interferometer. Measurement of the transverse resistance of a loop.

1.5 is nominated 'normal state quantum interferometer' since conductance vs flux oscillations result due to the interference between two electronic waves coming by upper and lower parts respectively. Depending on the value of the enclosed flux, the interference between the two paths can be either constructive or destructive, thus increasing or decreasing the probability of electron transfer from left to right.

Persistent current is an equilibrium current not decaying in time. In large systems, the magnitude of this current becomes unobservably small.

Persistent current is a sample sensitive phenomenon. Its value and even sign depends on properties such as position of specific impurities, number of electrons (odd or even), etc. Flux enters to the Hamiltonian through the phase increment between adjacent sites.

$$\alpha = \frac{2\pi}{N_a} \frac{\Phi}{\Phi_0} \quad (1.21)$$

where  $N_a$  is the number of atoms in a loop.

$$H = -t \sum_{n=1}^{N_a} a_n^\dagger a_{n+1} \exp(i\alpha) + a_{n+1}^\dagger a_n \exp(-i\alpha) \quad (1.22)$$

and

$$E_n = -2t \cos(K_n + \alpha) \quad (1.23)$$

If we include the effect of the impurities

$$H_I = V \sum_n \xi_n a_n^\dagger a_n \quad (1.24)$$

The solution of the problem is identical to the solution of the wave function in a crystal with a periodic potential. Allowance for elastic scattering changes the  $E(\Phi)$  dependence by opening a gap at  $\Phi = n\Phi_0$ .  $E(\Phi)$  dependence is similar to the energy (momentum) dependence in the extended zone scheme (the Bloch problem), see Figure 1.6.  $\Phi$  serves as quasi-momentum. Scattering of electrons does not result in decaying of current, as in the case of superconductivity. However the reasons for zero resistance in both cases are different. In a superconductor, current-carrying state is stabilized by virtue of finite binding of two electrons making a bosonic pair so called ‘Cooper pair’. In a nonsuperconducting metal there is no such binding, but the Aharonov-Bohm effect in combination with the energy quantization in macroscopically small and microscopically large (mesoscopic) system does the same. Scattering results in the redistribution of electrons over different states, yet total current remains nonzero. This is an exact statement. Therefore, due to Aharonov-Bohm effect, there appears a current which is nondecaying in time, a persistent current. Scattering influences the magnitude of the persistent current. The current oscillates as a function of magnetic flux with a period  $hc/e$  (flux quantum for normal, nonsuperconducting sample). If the ring is superconducting, it can carry a supercurrent. Unlike the persistent current, the latter persists in large system. Supercurrent state is metastable, but relaxation times of its decay are of cosmological value. In very small samples, decay time becomes measurable, and the system shows the characteristics of persistent current only. See the reference by I. O. Kulik<sup>47</sup> pages 2-14 and the references therein.

In the next section we briefly present some models of high- $T_c$  superconductivity. We use two of these models in chapter 2 and chapter 3.

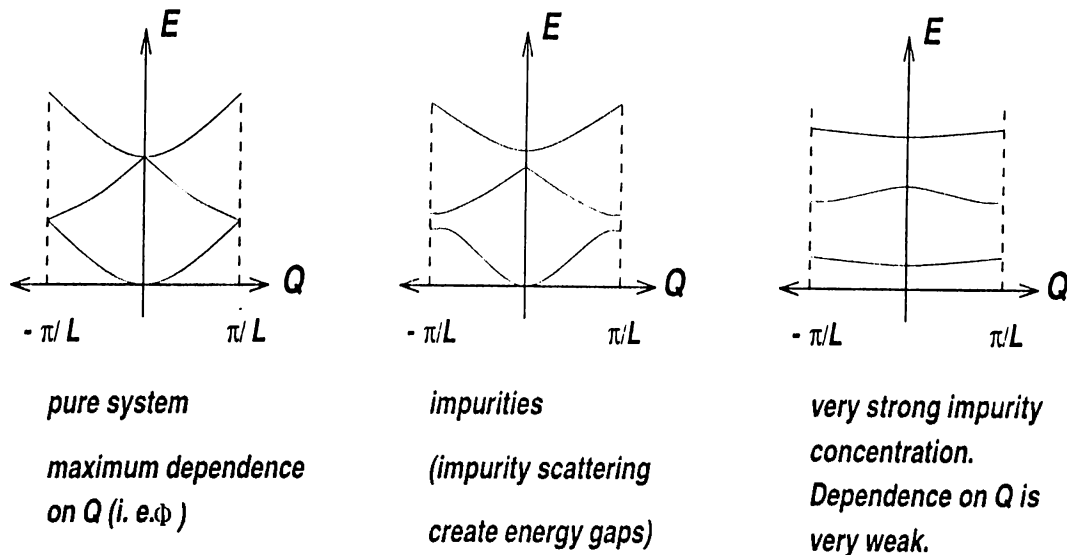


Figure 1.6: The effect of the impurities on the energy in the extended zone scheme.

### 1.3 Strongly Correlated Models of High- $T_c$ Superconductivity

The BCS theory<sup>35</sup> employs an effective interaction, energy transfer of order Debye frequency  $\omega_D$  in phonon exchange, and other simplifications. It is a quasiparticle description with a constant effective interaction. However, in reality the electron-phonon interaction causes a mass enhancement near the Fermi energy and a finite lifetime of a quasiparticle. With the excitation energy in the order of Debye frequency, the lifetime of a quasiparticle is short and its level width is of the order of the excitation energy. That is, its damping is very strong and a well-defined quasiparticle no longer exists. Hence, the quasiparticle picture becomes invalid. More detailed considerations of electron-electron interaction, frequency dependency in energy transfers, and other refinements are needed. The theory of strongly coupled superconductors was thus developed.<sup>40,55</sup>

Since the discovery of the phenomenon of superconductivity, constant effort has been made to search for a new material with a higher transition point.

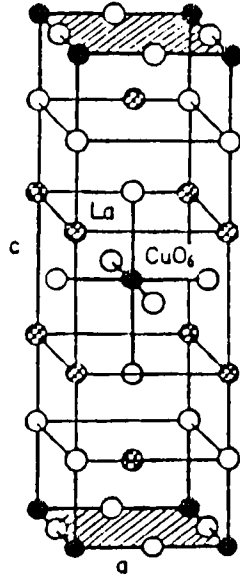
Nevertheless, even after more than a half century, the highest critical temperature until 1986 was still in the region of 20 K. It appeared as if the  $T_c$  of 23.3 K in  $Nb_3Ge$  was a limit. However, in the 75th anniversary year of superconductivity, that is in 1986, Bednorz and Müller<sup>36</sup> discovered that  $LaBaCuO$  can be a superconductor at 35 K. This was a total surprise not only because of high value of  $T_c$ , but because the compound is a ceramic and is entirely different from all the previously known superconducting materials. The discovery triggered an exciting search for new materials in the new domain, causing a flood of reports on the subject, including new materials with  $T_c$  as high as 90 K. The number of new materials has reached approximately forty. Below we present two representative families.

### (1) 2-1-4 compounds.

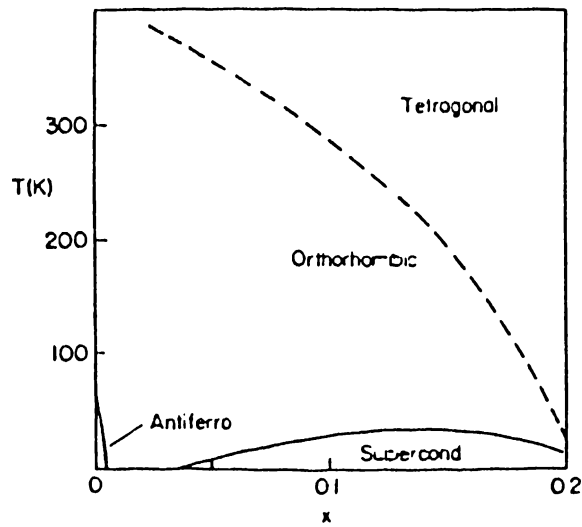
Related to the first high  $T_c$  superconductor is a family of compounds with the atomic structure  $La_{2-x}M_xCuO_{4-y}$ , where  $M$  is  $Ba$ ,  $Sr$ , or  $Ca$ ,  $x$  is of the order 0.15, and  $y$  is nearly zero. The family is commonly called the 2-1-4 copper oxide in correspondence to the atomic composition ratio of the basic case in which  $x = y = 0$ . This family has  $T_c$  of the order 40 K, and strontium appears to yield the highest.

Figure 1.7 shows the structure in which  $Cu$ ,  $O$  and  $La$  or  $M$  atoms are represented respectively by black, white and hatched circles. The  $Cu - O_2$  planes are hatched for distinction. With this layered structure the compounds are highly anisotropic, and superconductivity is associated with the  $Cu - O_2$  planes.

The compounds have the body centered tetragonal structure at high temperatures and the orthorhombic structure at low temperatures. These two structures and also the superconducting phase depend sensitively on oxygen doping. Figure 1.8 illustrates the phase diagram as a function of  $x$  in  $La_{2-x}Sr_xCuO_{4-y}$ . Below a certain temperature the orthorhombic phase is metallic, and above insulating. There is a tiny antiferromagnetic phase, which is enhanced as  $y$  is increased. The graph shows the plane at  $y = 0$ . The antiferromagnetic phase is insulating.



**Figure 1.7:** Crystal structure of  $La_2CuO_{4-y}$ . White Circles are oxygen atoms and black circles represent copper atoms, hatched circles represent lanthanum atoms.



**Figure 1.8:** Phase diagram of  $La_{2-x}Sr_xCuO_{4-y}$ .

The parent compound  $La_2CuO_{4-y}$  is not superconductive. In its ground state, the charges on  $La^{3+}$  and  $Cu^{2+}$  are balanced by  $O^{2-}$ . When doped with  $M$ , that is, in  $La_{2-x}M_xCuO_{4-y}$ , where  $M$  can be  $Sr$ , there are  $x - 2y$  holes per cell. These

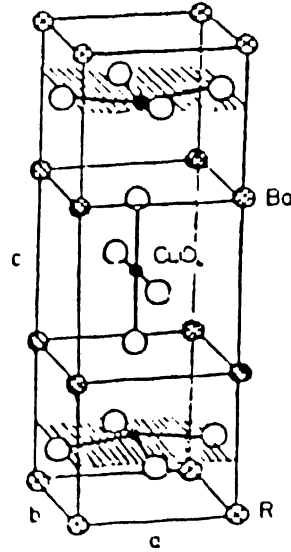


Figure 1.9: Structure of  $RBa_2Cu_3O_7$ .

Crossed circles at the corners of the unit cell of orthorhombic structure represent  $R$ , which can be  $Y$ ,  $Eu$ , etc. White circles are oxygen atoms.

holes are considered to go into  $O(2p)$  states and move about on each  $CuO_2$  plane.

## (2) 1-2-3 compounds

This family has the general structure  $RBa_2Cu_3O_{7-\delta}$ , where  $R$  is  $Y$ ,  $Eu$ ,  $Gd$  and so on. Figure 1.9 shows the structure. The  $Cu-O_2$  planes are hatched for clarity. Between these two planes are two  $Ba-O$  planes. Above  $500^\circ\text{C}$ , the insulating tetragonal phase is stable.

The phase diagram of  $YBa_2Cu_3O_{7-\delta}$  is shown in Figure 1.10 as a function of the oxygen content parameter  $\delta$ . Note that as  $\delta$  decreases, the hole concentration increases; the hole concentration is given by  $(1 - 2\delta)$  per cell. The critical temperature can be as high as 93 K for  $\delta = 0$ . The antiferromagnetic insulating phase appears when  $\delta$  is above around 0.7. Below this value, the compounds are metallic.

Both 1-2-3 and 2-1-4 compounds have an insulating antiferromagnetic phase below a certain temperature. The antiferromagnetic phase is due to the unpaired spins of copper electrons. Doping converts them into spin liquids, metals, and

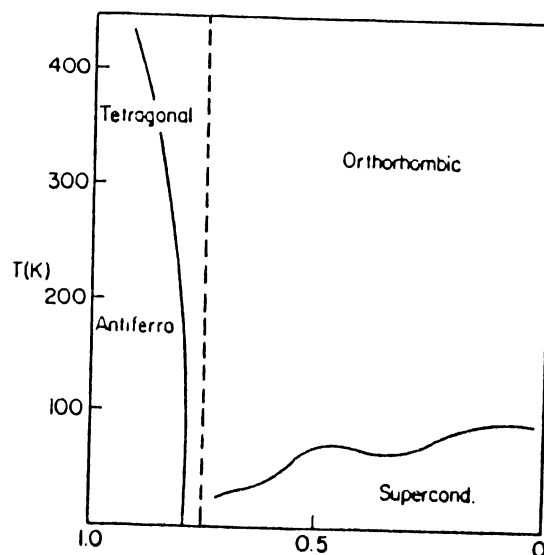
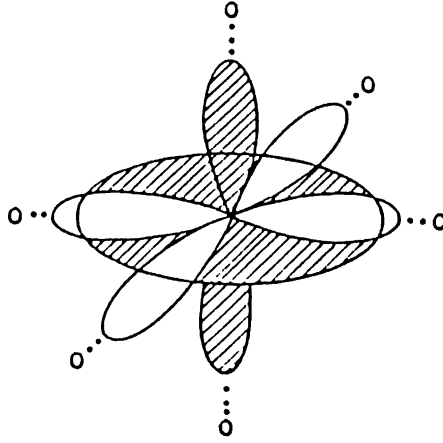


Figure 1.10: Phase diagram of  $YBa_2Cu_3O_{7-x}$ .

then superconductors.

The  $CuO_2$  planes play an important role for superconductivity, even though there are copperless materials. In fact, the critical temperature is sensitive to the oxygen atoms in these planes. Each copper atom has ten electrons in the  $3d$  shell, which consists of one  $d(x^2 - y^2)$  orbital and one  $d(z^2)$  orbital. The former has four lobes directed toward the four oxygen atoms in the same  $xy$  plane, while the latter has two lobes pointed to the two oxygen atoms above and below the plane and one circular orbital in the  $xy$  plane. The single  $4s$  electron and one of the ten  $3d$  electrons of copper hybridize with the oxygen  $2p$  electrons to form  $La_2CuO_4$ , keeping the  $d(x^2 - y^2)$  orbital partially empty while the  $d(z^2)$  orbital is filled. The remaining nine electrons in the  $d(x^2 - y^2)$  orbital invite oxygens in the same plane to come closer. On the other hand, the electrons in the filled  $d(z^2)$  orbital expel the oxygens above and below the  $xy$  plane. These configurations are illustrated in Figure 1.11 in which the  $d(z^2)$  orbital is shaded.

Note that eight of nine electrons in the  $Cu d(x^2 - y^2)$  are paired, while one is unpaired. Thus, at each  $Cu$  site there is a hole with a localized spin. Since the  $d(x^2 - y^2)$  orbital is strongly coupled with the  $O(2p)$  orbital, one can talk about



**Figure 1.11:** Copper d-orbitals.

The four lobes of  $d(x^2 - y^2)$  orbital are white and the  $d(z^2)$  orbital is hatched. The locations of the neighboring oxygen atoms are indicated. The top and bottom oxygens are at a greater distance than those on the horizontal plane.

$O(2p)$  or  $Cu(3d)$  holes.

The localized spin of the ninth, called  $d9$ , electron of copper causes antiferromagnetism. It is difficult for an unpaired spin to move about in an antiferromagnetic configuration due to energy costs. However, this configuration can easily be destroyed by doping or by some other disorder, particularly in two dimensions.

The replacement of  $La^{3+}$  by  $Sr^{2+}$  in  $La_{2-x}Sr_xCuO_{4-y}$  creates  $(x - 2y)$  holes per cell. The copper atoms appear to keep the same valance state,  $Cu^{2+}$ , even after doping. Hence, the holes seem to be on the oxygen sites, creating  $O^-$ . There are  $(1 - 2\delta)$  holes per cell in the 1-2-3 compounds  $RBa_2Cu_3O_{7-\delta}$  with  $R^{3+}$ . Accordingly, the 1-2-3 compounds can have more holes than the 2-1-4. Note that their critical points are also higher. Since the superconductive phase stretches beyond  $\delta = 0.5$ , some  $Cu^{2+}$  might be converted into  $Cu^+$  as the hole concentration in the plane increases.

It becomes easier for the holes on copper (or oxygen) sites to move about once

the antiferromagnetic regularity is destroyed. The high critical point indicates that a certain process involving high energy plays a role in pairing of holes. The destruction of the antiferromagnetic configuration by doping cannot be neglected in this respect, particularly because the resultant spin glass phase is not metallic but is insulating. The superconductive transition in the 2-1-4 compounds is preceded by an insulator-metal transition, but a direct transition from a spin glass state to a superconducting state without entering a metallic phase appears to take place in the 1-2-3 compounds near absolute zero.

The holes created by doping are primarily on the  $O^-$  sites in the  $Cu - O_2$  planes. In consideration of their hopping from site to site, including copper sites we express the Hamiltonian of a single  $Cu - O_2$  plane as follows:

$$H = \sum_{i,\sigma} \varepsilon_{ij} c_{i\sigma}^\dagger c_{j\sigma} + \frac{1}{2} \sum_{i,j,\sigma,\sigma'} U_{ij} c_{i\sigma}^\dagger c_{i\sigma} a_{j\sigma'}^\dagger c_{j\sigma'} \quad (1.25)$$

The operator  $c_{i\sigma}^\dagger$  creates a hole with spin  $\sigma$  in the  $2p_x$  or  $2p_y$  orbital at the copper site  $i$ . The hole is in the  $3d(x^2 - y^2)$  orbital of copper. The diagonal energies will be either  $(\varepsilon_p, U_p)$  or  $(\varepsilon_d, U_d)$  for the  $2p$  or  $3d$  state respectively.

The choices

$$\begin{aligned} \varepsilon_{ij} &= -t \\ U_{ij} &= U \end{aligned}$$

simplify the Hamiltonian. In addition, if

$$\begin{aligned} U_p &= U_d = U \\ U_{pd} &= 0 \end{aligned}$$

the above Hamiltonian is reduced to a single band Hubbard Hamiltonian:

$$H = -t \sum_{(ij)} c_{i\sigma}^\dagger c_{j\sigma} + U \sum_j n_{j\uparrow} n_{j\downarrow} \quad (1.26)$$

The same Hamiltonian can of course describe electron hopping. Its properties depend on the relative strength of  $t$  and  $U$ . The first term represents hopping

between neighboring sites ( $ij$ ), and the second term represents the interaction at the same site  $j$ . If this interaction is repulsive and large such that  $U \gg t$ , no two electrons can be on the same site. Hence, each site is taken by only a single electron with a certain spin. As a consequence, the electrons can hardly move. Due to large  $U$ , the band is split into two with a gap between. That is, a half filled Hubbard model corresponds to an insulator with an energy gap between the lower occupied and upper unoccupied states. Thus, this Hamiltonian may be adopted for the insulating phase of high  $T_c$  materials.

It is convenient to start with the above Hamiltonian, not distinguishing the copper and oxygen sites from each other. However, the single band model is symmetric under a particle-hole transformation. Thus, removing holes from the  $Cu - O_2$  planes is equivalent to adding them. This symmetry can be broken by a more elaborate *copper-oxygen model*. In this model, the removal of holes from the copper sites produces  $Cu^+$ . The energy of  $Cu^+$  can be higher or lower than  $\varepsilon_d$  of  $Cu^{2+}$ . If it is higher, and if oxygen's  $\varepsilon_p$  is located between the two energies, any additional hole will go into oxygen sites. Only in the opposite case, in which  $\varepsilon_d$  is higher than  $\varepsilon_p$ , can the holes go into the copper sites. Spectroscopic observations of excess holes on oxygen sites favor the copper-oxygen model. These excess holes are the charge carriers.

Doping supplies additional oxygens and weakens magnetic coupling. Thus spin flipping takes place, causing local spin-parallel configurations. This occurrence can be seen by examining the interaction of spins  $\mathbf{S}_1$  and  $\mathbf{S}_2$  on the neighboring  $Cu^{2+}$  with spin  $\sigma$  of an oxygen hole:

$$H = -J(\mathbf{S}_1 + \mathbf{S}_2) \cdot \sigma \quad (1.27)$$

In order to minimize this energy,  $\sigma$  prefers to be parallel (antiparallel) to both  $\mathbf{S}_1$  and  $\mathbf{S}_2$  if  $J > 0$  ( $J < 0$ ). That is, regardless of the sign of  $J$ ,  $\mathbf{S}_1$  and  $\mathbf{S}_2$  are preferably parallel. Moreover, since the oxygen hole is presumably located closer to copper than the original  $Cu - O$  distance, the above energy would overcome the antiferromagnetic energy.

The local parallel-spin configurations created by doping stir up spin

frustration, so that the material becomes a quantum spin liquid. This liquid state is insulating, but may be considered as a parent state for superconductivity. Note that the ground state of a 1d Bethe lattice corresponds to a spin liquid. On the other hand, Raman scattering studies<sup>31</sup> have revealed that spin fluctuations in nonsuperconducting  $La_2CuO_4$  are characterized by an extremely high exchange constant  $J \sim 1100 \text{ cm}^{-1} = 137 \text{ meV}$ . A similar magnitude  $J \sim 950 \text{ cm}^{-1}$  has been found in  $YBa_2Cu_3O_{7-\delta}$ . Therefore energies of order 1000 K may be involved for pairing. Increasing the oxygen concentration causes broadening and weakening of the spin pair peak and dilution of the spin system in the planes. That is, spins are removed as the oxygen concentration is increased. This indicates that magnon exchange may not be responsible for pairing. In fact, there are perovskites such as  $BaPbO_3$  that do not show any special magnetic properties, but have  $T_c$  of the order 30 K. It is also known that the excitations from the Bethe state are not spin waves but are quasi-fermions called spinons.

The existence of the  $O - Cu - O$  configuration before doping requires a close examination of energy changes due to excess oxygen atoms in relation to their motion in the  $Cu - O_2$  planes. For instance, Emery and Reiter<sup>41</sup> solved a model in which an oxygen hole moves through a ferromagnetic copper spin background. This model suggests that pairing of these holes is mediated by enhanced superexchange coupling.

On the other hand, noting that a metal-insulator transition is close to the superconducting transition, Anderson<sup>44</sup> suggested that the insulating phase is an RVB (resonating valence band state). With sufficient doping, the magnetic singlet pairs in the insulating state become charged superconducting pairs. His model may be described in a simple way by starting with a half-filled Mott insulator in a simple square lattice. This system corresponds to a Heisenberg antiferromagnet and is represented by the Hamiltonian

$$H = J \sum_{\langle ij \rangle} (\mathbf{S}_i \cdot \mathbf{S}_j) - \frac{1}{4} \quad (1.28)$$

In terms of Hubbard's  $t$  and  $U$  the exchange constant  $J = 4t^2/U$ . The spin

operators can be rewritten in terms of the electron operators such that

$$H = -J \sum_{\langle ij \rangle} b_{ij}^\dagger b_{ij} \quad (1.29)$$

with the local constraints  $n_{i\uparrow} + n_{i\downarrow} = 1$ . Here the singlet operators  $b_{ij}^\dagger$  are defined by

$$b_{ij}^\dagger = \frac{1}{\sqrt{2}}(c_{i\uparrow}^\dagger c_{j\downarrow}^\dagger - c_{i\downarrow}^\dagger c_{j\uparrow}^\dagger) \quad (1.30)$$

It is interesting that the new Hamiltonian has the local gauge symmetry for  $c_{i\sigma}^\dagger \rightarrow \exp(i\theta)c_{i\sigma}^\dagger$ . A similar gauge symmetry has been discussed for the fractional quantum Hall effect. The spins behaving as fermions are spinons. If an electron is removed by doping a hole, called holon, is created. The holons do not carry spins but only charges. The effective Hamiltonian for a doped material can be expressed in terms of holon and spinon operators of the BCS case. At temperatures below  $J \sim 1000$  K, the spinons do not hop. The dominant process is tunneling of a holon pair, which involves a virtual excitation of a spinon.

In the investigation of unusual electronic properties of metal-oxide, compounds it was proposed<sup>45,50</sup> that the new features in the electronic band conduction should be included. The first is the possibility that intrinsic-hole rather than intrinsic-electron carriers may ply the game. The second one is that, provided 'intrinsic-holes' are at work, one-particle picture of the electronic transport is not fully adequate. Because the interaction between holes (repulsive or attractive) has to be included, and the fact that hopping of holes in itself cannot be considered as a constant and is strongly dependent upon site occupation should be taken into account. Hence, anion network in the  $CuO_2$  plane of metal-oxide compound is considered<sup>51</sup> as an intrinsic-hole metal with holes rather than electrons comprising a Fermi liquid immersed in the background of negative  $O^{2-}$  ions. Due to the contraction of  $p$ -orbital of oxygen as a result of occupation by a hole, hole hopping between nearest neighbor sites ( $i, j$ ) is dependent upon opposite-spin hole occupation number. It has been proposed to consider, in the second quantization representation, the hopping matrix element  $t_{ij}$  as an operator depending on the occupation operators  $n_i$  and  $n_j$  of the atomic sites  $R_i$  and  $R_j$ .<sup>48</sup>

There are three independent matrix elements  $t_0$ ,  $t_1$ , and  $t_2$ <sup>49,60</sup> corresponding to, in the case of two oxygen anions

$$\begin{aligned} t_0 : O_i^- + O_j^{2-} &\Rightarrow O_i^{2-} + O_j^- \\ t_1 : O_i + O_j^{2-} &\Rightarrow O_i^{2-} + O_j \\ t_2 : O_i + O_j^- &\Rightarrow O_i^- + O_j \end{aligned} \quad (1.31)$$

which result in

$$\begin{aligned} t_{ij} = & t_0(1 - n_{i,-\sigma})(1 - n_{j,-\sigma}) + t_1[n_{i,-\sigma}(1 - n_{j,-\sigma}) + n_{j,-\sigma}(1 - n_{i,-\sigma})] + \\ & t_2 n_{i,-\sigma} n_{j,-\sigma} \end{aligned} \quad (1.32)$$

The occupation dependence of the hopping can be represented in another form:

$$t_{ij} = -t + V n_{i,-\sigma} n_{j,-\sigma} + W(n_{i,-\sigma} + n_{j,-\sigma}) \quad (1.33)$$

where from Eq. (1.31)

$$t = -t_0, \quad V = t_0 - 2t_1 + t_2, \quad W = t_1 - t_0 \quad (1.34)$$

Hence, 1d version of interacting holes in an anion network is represented by Hamiltonian including, along with the contraction interaction, the Hubbard term

$$\begin{aligned} H = & - \sum_{i,\sigma} c_{i,\sigma}^\dagger c_{i+1,\sigma} \exp(i\alpha) + h.c. + U \sum_i n_{i,\uparrow} n_{i,\downarrow} \\ & + \sum_{i,\sigma} c_{i,\sigma}^\dagger c_{i+1,\sigma} [V n_{i,-\sigma} n_{i+1,-\sigma} + W(n_{i,-\sigma} + n_{i+1,-\sigma})] \exp(i\alpha) + h.c. \end{aligned} \quad (1.35)$$

The effect of coupling term  $W$  has been considered in much detail in the paper of Hirsch and Marsiglio,<sup>7</sup> as well as of I. O. Kulik.<sup>49,50</sup> Both types of the contraction pairing are considered.<sup>51</sup>

Our model Hamiltonian in chapter 2 will be that of Eq. (1.26), and in chapter 3, it will be that of Eq. (1.35).

In addition to above three models there are several other models. However, a convincing description at a finite value of doping is still lacking and the basic mechanism is yet to be disclosed. For further reading see section 7.2 of *High-Temperature Superconductors* by N. M. Plakida<sup>10</sup> and the references therein.

# Chapter 2

## 1-D HUBBARD MODEL

We consider a loop of  $N_a$  lattice sites, which in fact is equivalent to a one dimensional chain, with a total number of  $N_e$  electrons. We will assume that there is a magnetic flux  $\Phi$  through the loop. Suppose that electrons can hop between neighboring lattice sites, and at each site at most two electrons with opposite spins can sit together with an interaction energy  $U$ . The Hamiltonian for this system has the following form:

$$H = -t \sum_{i,\sigma} (c_{i,\sigma}^\dagger c_{i+1,\sigma} e^{i\alpha} + c_{i+1,\sigma}^\dagger c_{i,\sigma} e^{-i\alpha}) + U \sum_i n_{i,\uparrow} n_{i,\downarrow} \quad (2.1)$$

where  $c_{i,\sigma}^\dagger$  and  $c_{i,\sigma}$  are, respectively, the creation and annihilation operators for an electron of spin projection  $\sigma$  at the  $i^{\text{th}}$  lattice site;  $t$  is the electron hopping amplitude;  $\alpha = \frac{2\pi}{N_a} \frac{\Phi}{\Phi_0}$  where  $\Phi_0 = \frac{hc}{e}$  is the magnetic flux quantum;  $n_{i,\sigma}$  is the occupation number operator. The energy spectrum of  $H$  is invariant under the replacement of  $t$  by  $-t$ . So, we will take  $t = +1$  in appropriate units.

The lattice sites of the loop can be numbered from 1 to  $N_a$ . Hence we use the following wave function for the system:

$$|\Psi\rangle = \sum_{x_1, x_2, \dots, x_{N_e}} f(x_1, \dots, x_{M+1}, \dots, x_{N_e}) c_{x_1, \uparrow}^\dagger \dots c_{x_{M+1}, \uparrow}^\dagger \dots c_{x_{N_e}, \downarrow}^\dagger |0\rangle \quad (2.2)$$

Here,  $f(x_1, \dots, x_{N_e})$  represents the amplitude in the coordinate representation for which the down spin electrons are at sites  $x_1, \dots, x_M$  and up spin electrons

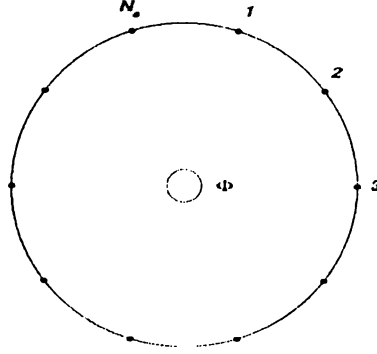


**Figure 2.1:** Sample configuration

There are  $N_a$  lattice sites on the ring which can be numbered from 1 to  $N_a$ . The flux  $\Phi$  piercing the ring is produced by a solenoid inserted in the ring.

are at sites  $x_{M+1}, \dots, x_{N_e}$  ( $M$  is the number of electrons with spin projection down and  $N_e - M$  is the number of electrons with spin projection up). The amplitude function has the following symmetry property:  $f(x_1 + N_a, x_2 \dots x_{N_e}) = f(x_1, x_2 + N_a \dots x_{N_e}) = \dots = f(x_1, x_2 \dots x_{N_e} + N_a) = f(x_1, x_2 \dots x_{N_e})$ . Using the commutation relation for fermions, which is  $[c_{i,\sigma}, c_{j,\sigma'}^\dagger]_+ = \delta_{i,j} \delta_{\sigma,\sigma'}$ , and the definition of occupation number operator  $n_{i,\sigma} = c_{i,\sigma}^\dagger c_{i,\sigma}$ , the eigenvalue equation  $H|\Psi\rangle = E|\Psi\rangle$  leads to:

$$\begin{aligned}
 & - \sum_{i=1}^{N_e} f(x_1, x_2, \dots, x_i + 1, \dots, x_{N_e}) e^{i\alpha} + f(x_1, x_2, \dots, x_i - 1, \dots, x_{N_e}) e^{-i\alpha} + \\
 & U \sum_{i=1}^M \sum_{j=M+1}^{N_e} \delta(x_i - x_j) f(x_1, x_2, \dots, x_{N_e}) = E f(x_1, x_2, \dots, x_{N_e}) \quad (2.3)
 \end{aligned}$$

where

$$\begin{aligned}
 x_1 &= 1, 2, \dots, N_a \\
 x_2 &= 1, 2, \dots, N_a \\
 &\vdots \\
 x_{N_e} &= 1, 2, \dots, N_a
 \end{aligned}$$

and,

$$\delta(x_i, x_j) = \begin{cases} 1 & \text{if } x_i = x_j \\ 0 & \text{if } x_i \neq x_j \end{cases} \quad (2.4)$$

Note that,  $N_e$  electrons in the non-interacting lattice ( $U = 0$ ) have an energy eigenvalue  $E^{(0)} = -2 \sum \cos(k_j + \alpha)$ , where the momenta of the  $N_e$  electrons are,  $k_j = \frac{2\pi}{N_a} n_j$ , and  $n_j = 1, \dots, N_a$ . This shows that energy of non-interacting electron system has  $hc/e$  periodicity.

## 2.1 Ground State Energy of Two Electrons

The wave function for two electrons, one with spin up the other with spin down, will be the following:

$$|\Psi\rangle = \sum_{x_1, x_2} f(x_1, x_2) c_{x_1}^\dagger c_{x_2}^\dagger |0\rangle \quad (2.5)$$

The eigenvalue equation  $H|\Psi\rangle = E|\Psi\rangle$  leads to

$$-[(f(x_1 + 1, x_2) + f(x_1, x_2 + 1)) \exp(i\alpha) + (f(x_1 - 1, x_2) + f(x_1, x_2 - 1)) \exp(-i\alpha)] + U\delta(x_1, x_2)f(x_1, x_2) = Ef(x_1, x_2) \quad (2.6)$$

We can transform the above equation to momentum representation with the following substitutions:

$$\delta(x_1, x_2) = \frac{1}{N_a} \sum_K \exp(iK(x_1 - x_2)) \quad (2.7)$$

where  $K = \frac{2\pi}{N_a} n$ ,  $n = 0, 1, 2, \dots, N_a - 1$ , and

$$f(x_1, x_2) = \sum_{K_1, K_2} f_{K_1, K_2} \exp(iK_1 x_1) \exp(iK_2 x_2), \quad (2.8)$$

where  $K_{1,2} = \frac{2\pi}{N_a} n_{1,2}$ ,  $n_{1,2} = 0, 1, 2, \dots, N_a - 1$ . Here  $f_{K_1, K_2}$  is assumed to satisfy the periodicity condition  $f_{K_1+2\pi, K_2} = f_{K_1, K_2+2\pi} = f_{K_1, K_2}$ . After some calculations we get the following simplified equation for  $f_{K_1, K_2}$

$$(E + 2 \cos(K_1 + \alpha) + 2 \cos(K_2 + \alpha)) f_{K_1, K_2} = \frac{U}{N_a} \sum_K f_{K_1-K, K_2+K} \quad (2.9)$$

so that

$$f_{K_1, K_2} = \frac{\frac{U}{N_a} \sum_K f_{K_1-K, K_2+K}}{E + 2 \cos(K_1 + \alpha) + 2 \cos(K_2 + \alpha)} \quad (2.10)$$

After a second summation we get

$$\frac{1}{N_a} \sum_p f_{K_1-p, K_2+p} = \frac{U}{N_a} \sum_p \frac{\frac{1}{N_a} \sum_K f_{K_1-K-p, K_2+K+p}}{E + 2 \cos(K_1 - p + \alpha) + 2 \cos(K_2 - p + \alpha)} \quad (2.11)$$

Realizing the fact that  $\frac{1}{N_a} \sum_K f_{K_1-K, K_2+K} \equiv \Phi_Q$  is only a function of  $Q = K_1 + K_2$  in mod  $2\pi$ , we arrive at

$$\Phi_Q \left( 1 - \frac{U}{N_a} \sum_p \frac{1}{E + 2 \cos(K_1 - p + \alpha) + 2 \cos(K_2 + p + \alpha)} \right) = 0 \quad (2.12)$$

Hence, either the term inside the parenthesis or  $\Phi_Q$  is equal to zero.

(1)  $\Phi_Q \neq 0$  case.

$$\frac{1}{U} = \frac{1}{N_a} \sum_p \frac{1}{E + 2 \cos(K_1 - p + \alpha) + 2 \cos(K_2 + p + \alpha)} \quad (2.13)$$

or shortly

$$\frac{1}{U} = S(E) \quad (2.14)$$

The above transcendental equation can be solved numerically and the value of the energy  $E$  can be found. The points where  $S(E)$  intersects with  $\frac{1}{U}$  are the eigenvalues  $E$  of the system (see Fig. (2.2)). The flux dependence of the energy, related to Eq. (2.14), is presented in Fig. (2.5).

We can apply Poisson summation formula,

$$\sum_{n=n_1}^{n_2} f(n) = \sum_{s=-\infty}^{\infty} \int_{n_1}^{n_2} f(n) \exp(2\pi i n s) dn \quad (2.15)$$

to Eq. (2.13) and we get

$$\frac{1}{U} = \sum_{s=-\infty}^{\infty} \int_0^{2\pi} \frac{dp}{2\pi} \frac{\exp(ipN_a s)}{E + 2 \cos(Q/2 - p) \cos(Q/2 + \alpha)} \quad (2.16)$$

So  $S(E)$  becomes

$$S(E) = \sum_{s=-\infty}^{\infty} S_s(E) \equiv S_{s=0}(E) + \sum_{s=1}^{\infty} S_s(E) + S_s^*(E) \quad (2.17)$$

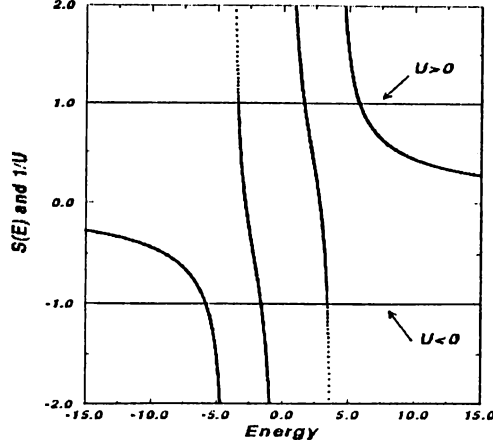


**Figure 2.2:** Plot of transcendental equation for 1-d Hubbard model with 2 electrons.

The points where  $S(E)$  intersects with  $\frac{1}{U}$  are the eigenvalues  $E$  of the system. Here  $N_a = 4$ ,  $Q = 0$ ,  $\alpha = 0$ .

We can calculate  $S_s(E)$  in the complex plane. Let  $z = e^{ip}$  then  $dz = iz dp$ ,

$$S_s(E) = \frac{1}{2\pi i} \oint dz \frac{z^{N_a s}}{z^2(e^{i\alpha} + e^{-i(Q+\alpha)}) + Ez + (e^{i(Q+\alpha)} + e^{-i\alpha})} \quad (2.18)$$

This integral can be calculated with the use of the residue theorem. The poles of the denominator are

$$z_{1,2} = -\frac{-E \pm \sqrt{E^2 - E_0^2}}{E_0 \exp(-iQ/2)} \quad (2.19)$$

where  $E_0 = 4 \cos(Q/2 + \alpha)$ . For  $E^2 < E_0^2$ , both of the poles  $z_1$  and  $z_2$  are on the unit circle, while for  $E^2 > E_0^2$  one of them is inside, the other one is outside of the unit circle. The only difference between these two cases is that,  $S_{s=0}$  term vanishes for  $E^2 < E_0^2$ , while the same term survives for the other one.

For both possibilities we get the following result

$$S(E) = \frac{1}{4i \sin x \cos \beta} \frac{\exp(i(Q/2 - k)N_a) + 1}{\exp(i(Q/2 - k)N_a) - 1} \quad (2.20)$$

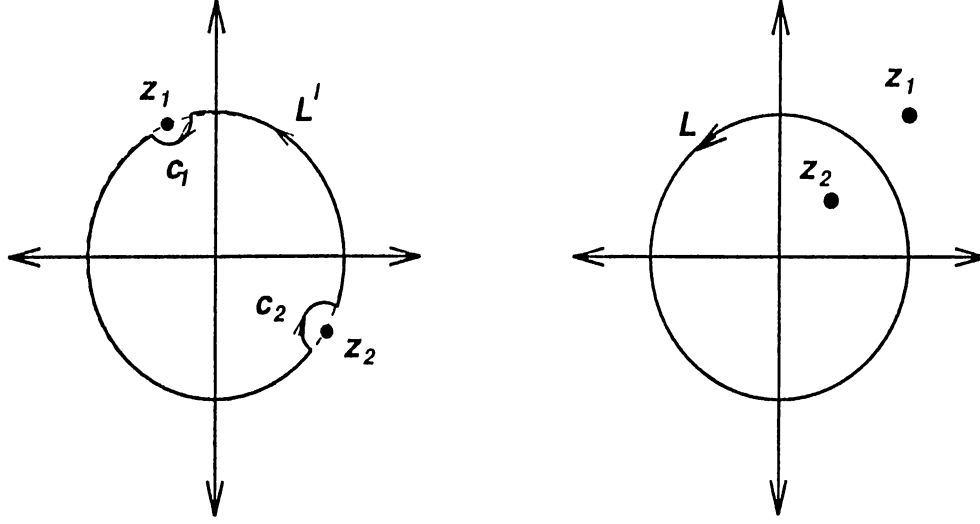


**Figure 2.3:** The poles of the integral in the complex plane.

For  $E^2 < E_0^2$ , both of the poles are on the unit circle, while for  $E^2 > E_0^2$ , one of them is inside, the other is outside of the unit circle.

where

$$x = \begin{cases} \kappa & \text{if } E^2 < E_0^2 \\ i\kappa & \text{if } E^2 > E_0^2 \end{cases} \quad (2.21)$$

and

$$\beta = Q/2 + \alpha \quad (2.22)$$

If we denote new momenta as

$$k_1 = \frac{Q}{2} + \alpha + x \quad (2.23)$$

$$k_2 = \frac{Q}{2} + \alpha - x \quad (2.24)$$

we get

$$\exp(i(k_1 - \alpha)N_a) = \frac{\sin k_1 - \sin k_2 + iU/2}{\sin k_1 - \sin k_2 - iU/2} \quad (2.25)$$

and

$$\exp(i(k_2 - \alpha)N_a) = \frac{\sin k_2 - \sin k_1 + iU/2}{\sin k_2 - \sin k_1 - iU/2} \quad (2.26)$$

With the substitution

$$\Lambda = \frac{\sin k_1 + \sin k_2}{2} \quad (2.27)$$

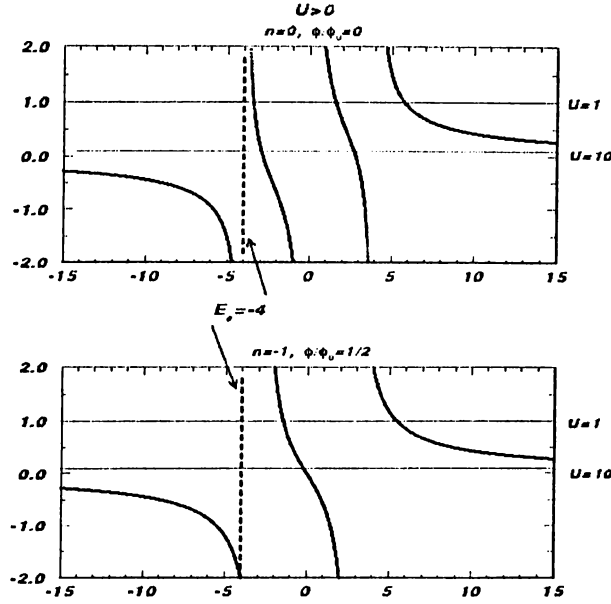


**Figure 2.4:** Plot of the transcendental equation for  $U > 0$

When  $U > 0$ ,  $E^2$  is always less than  $E_0^2$ . The intersection of  $S(E)$  with  $1/U$  is always to the right of  $E_0$ .

and  $u = U/4$ , the Eqs. (2.25) and (2.26) take the following form

$$\exp(i(k_1 - \alpha)N_a) = \frac{\sin k_1 - \Lambda + iu}{\sin k_1 - \Lambda - iu} \quad (2.28)$$

and

$$\exp(i(k_2 - \alpha)N_a) = \frac{\sin k_2 - \Lambda + iu}{\sin k_2 - \Lambda - iu} \quad (2.29)$$

We will see in the next section that, Eqs. (2.28) and (2.29) are identical to the discrete Bethe Ansatz equations for two electrons.

As it is seen in Fig. (2.4), when  $U > 0$ ,  $E^2$  is always less than  $E_0^2$ . On the other hand, for  $U < 0$  there are two possibilities: (i) if the value of  $n$  is even, then for all values of  $U$ , the inequality  $E^2 > E_0^2$  is always satisfied; (ii) if  $n$  is odd, then  $E^2 > E_0^2$  is not always satisfied. In this case, the absolute value of  $U$  should be large enough, otherwise, just as in the case of  $U > 0$ ,  $E^2$  becomes

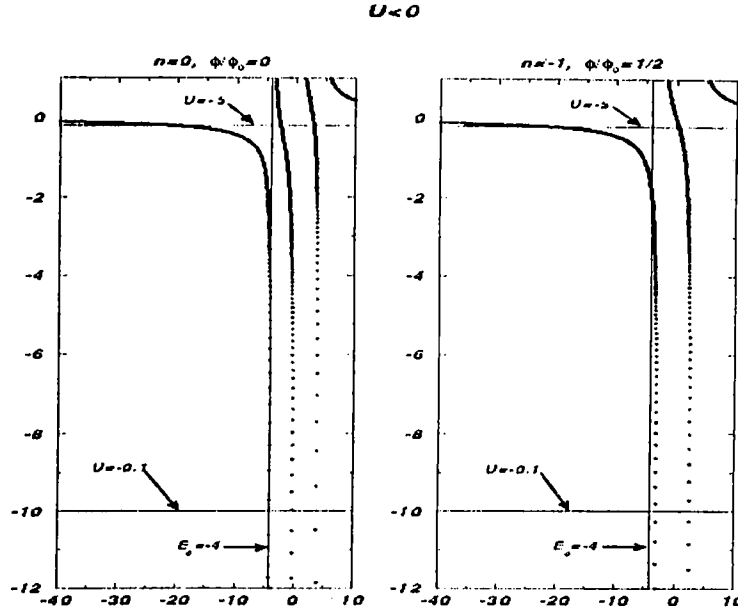


**Figure 2.5:** The plot of the transcendental equation for  $U < 0$ . When  $U < 0$   $E^2$  is not always larger than  $E_0^2$ . The intersection of  $S(E)$  with  $1/U$  is sometimes left to sometimes right to  $E_0$ , depending on the value of  $|U|$ .

smaller than  $E_0^2$ . It can be observed that, for odd values of  $n$ ,  $E^2$  is always larger than  $\cos^2(Q/2 - K)E_0^2$ , not  $E_0^2$ !

Let us try to find out the explicit forms of Eqs. (2.25) and (2.26). Let

$$s = 2 \frac{\sin k_1 - \sin k_2}{U} \quad (2.30)$$

so that

$$\exp(i k_1 N_a) = \exp(i \alpha N_a) \frac{s + i}{s - i} \quad (2.31)$$

Using the identity

$$\frac{s + i}{s - i} = -\exp(-2i \arctan s) \quad (2.32)$$

we get the following equations for  $k_1$  and  $k_2$

$$k_1 N_a = (2n_1 + 1)\pi + \alpha N_a - 2 \arctan \left( \frac{4 \sin x \cos \beta}{U} \right) \quad (2.33)$$

$$k_2 N_a = (2n_2 + 1)\pi + \alpha N_a - 2 \arctan \left( -\frac{4 \sin x \cos \beta}{U} \right) \quad (2.34)$$

where  $n_1$  and  $n_2$  are integers.

If we add the two equations, we find that  $(Q+2\alpha)N_a = (n_1+n_2+1)2\pi+2\alpha N_a$ . Hence we get a relation between all  $n$ 's:  $n_1 + n_2 + 1 = n$  (remember that  $Q = \frac{2\pi}{N_a} n$ ). Subtracting the equation governing  $k_2$  from the first one and dividing the result by four we get

$$\frac{N_a x}{2} = (n_1 - n_2) \frac{\pi}{2} - \arctan \left( \frac{4 \sin x \cos \beta}{U} \right) \quad (2.35)$$

Hence, it is possible to express the eigenvalue,  $E$ , of the system as

$$E = -4 \cos x \cos \beta \quad (2.36)$$

with  $x$  determined by

$$\tan \frac{N_a x}{2} = -\sigma \left( \frac{4 \sin x \cos \beta}{U} \right)^\sigma \quad (2.37)$$

where  $\sigma = +1$  for odd value of  $n$  and  $\sigma = -1$  for even value of  $n$ . Put  $x = \kappa$  for  $E^2 < E_0^2$ , and  $x = i\kappa$  for  $E^2 > E_0^2$ , where  $\kappa$  is a real quantity. Using above equations, it is possible to plot the ground-state energy as a function of flux. The results are exactly the same as those found by numerically solving Eq. (2.13) (see Fig. (2..)).

(2)  $\Phi_Q = 0$  case.

If  $\Phi_Q$  is equal to zero, we see from Eq. (2.9) that:

$$(E + 2 \cos(K_1 + \alpha) + 2 \cos(K_2 + \alpha)) f_{K_1, K_2} = 0 \quad (2.38)$$

To have  $\Phi_Q$  equal to zero, the sum of the  $f_{K_1, K_2}$ 's should be zero. But all of the  $f_{K_1, K_2}$ 's can not be equal to zero, otherwise  $|\Psi\rangle$  becomes zero. It is possible to show that we can put  $\sum_K f_{k_1-K, k_2+K}$  equal to zero only if for some two different combinations of  $(K_1, K_2)$ , the quantities  $2 \cos(K_1 + K + \alpha) + 2 \cos(K_2 - K + \alpha)$  are equal to each other. Otherwise, all  $f_{K_1, K_2}$ 's should be equal to zero which in turn

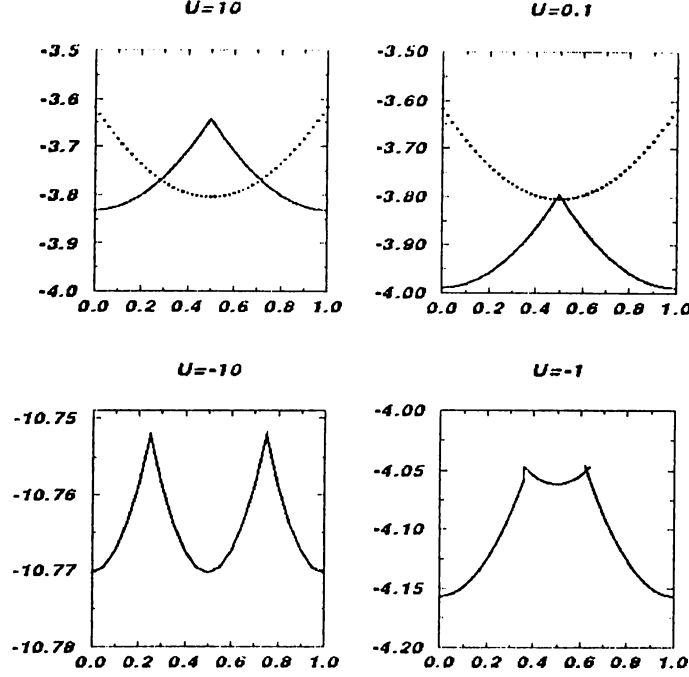


**Figure 2.6:** Energy versus flux for two electrons.

If the  $\Phi_Q = 0$  case is taken into account, new branches, which are the dotted lines for positive  $U$ , appear. This branch does not appear for negative  $U$ , since it is above the branch of first possibility. In short the new branch corresponding to the  $\Phi_Q = 0$  results in period halving for  $U > 0$ . The solution due to transcendental equation (Eq. (2.13)) and the analytical expression (Eq. (2.31)) are the same. In all the above graphs  $N_a = 10$ . We present the behavior of energy for both small and large values of  $U$ . For large enough  $|U|$  when  $U < 0$ , the minimum corresponding to  $\Phi/\Phi_0 = 1/2$  is almost equal to the one when  $\Phi/\Phi_0 = 0$  or 1. But when  $|U|$  gets smaller, this property vanishes, and the plot becomes similar to  $U = 0$  case, in which there is only  $\Phi_0$  periodicity.

means that  $|\Psi\rangle$  is zero. If the above requirement is fulfilled then the eigenvalue of the system becomes:

$$E = -2 \cos(q + \alpha) - 2 \cos(Q - q + \alpha) \quad (2.39)$$

with  $K_1 = q$  and  $K_2 = Q - q$ . Further consideration shows that when  $U > 0$ ,

and  $n$  is odd the minimum energy of the system becomes (see Fig. (2.6))

$$E = -4 \cos \frac{\pi}{N_a} \cos\left(\frac{Q}{2} + \alpha\right) \quad (2.40)$$

It can easily be seen that if this second possibility is not included, the number of eigenvalues is less than it should, that is the set of solutions is incomplete.

Equations (2.28) and (2.29) at  $\alpha = 0$  coincide with the Lieb and Wu solution<sup>52</sup> of 1-d Hubbard model for two electrons. The parameter  $\alpha$  generalizes this solution to the case of nonzero flux in the ring. Our analysis show that the Lieb and Wu solution is incomplete, because Eq. (2.41) also determines possible values of the energy available for two electrons in the ring. This extra solution is  $\alpha$  dependent and therefore it changes whence flux in the ring is changed.

### 2.1.1 The Dependence of Amplitude of Energy Oscillations on the Number of Sites

We investigate  $\Delta E(N)$  in two different cases:  $U > 0$  and  $U < 0$ .

(i)  $U > 0$

It is necessary to find out the value of  $\alpha_1$  (Fig. (2.7)) in order to determine  $\Delta E_1$  and  $\Delta E_2$ . With some simple algebra we find out the equation governing  $\alpha_1$

$$\frac{U}{4} = \tan \left[ \frac{N_a}{2} \arccos \left( \cos \frac{\pi}{N_a} \frac{\cos(\alpha_1 - \frac{\pi}{N_a})}{\cos \alpha_1} \right) \right] \sqrt{\cos^2 \alpha_1 - \cos^2 \frac{\pi}{N_a} \cos^2(\alpha_1 - \frac{\pi}{N_a})} \quad (2.41)$$

In the limit  $N_a \gg 1$

$$\alpha_1 \rightarrow \frac{1}{4} \frac{2\pi}{N_a} = \frac{\pi}{2N_a} \quad (2.42)$$

Hence substituting this value, we find out  $\Delta E_1$  and  $\Delta E_2$  as follows,

$$\Delta E_1 \approx \frac{1}{2} \frac{\pi^2}{N_a^2} \quad (2.43)$$

$$\Delta E_2 \approx \frac{1}{2} \frac{\pi^2}{N_a^2} \quad (2.44)$$

Both  $\Delta E_1$  and  $\Delta E_2$  behaves like  $\frac{1}{N_a^2}$ , and  $\frac{\Delta E_1}{\Delta E_2} \rightarrow 1$  for  $N_a \gg 1$ .

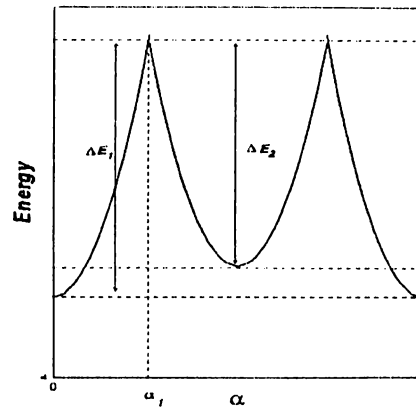


Figure 2.7: The energy oscillations for 2 electrons.

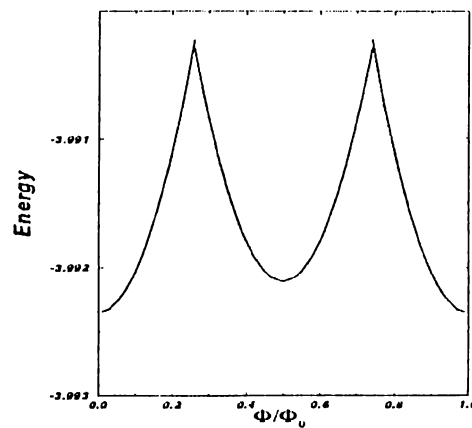
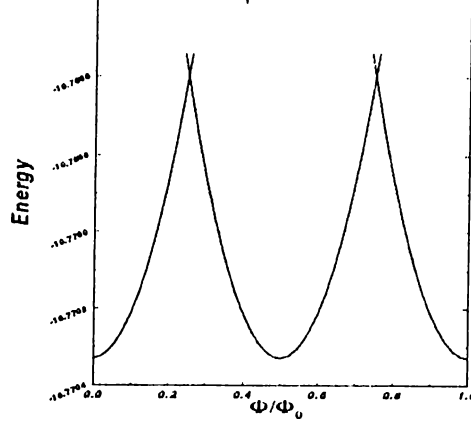


Figure 2.8: The energy oscillations for  $U > 0$  for  $N_a = 50$

(ii)  $U < 0$

In all the following calculations  $|U|$  is considered to be large enough. This time, For  $U < 0$  the calculations are easier, since with large  $N_a$  both  $\tanh \frac{N_a \alpha}{2}$  and



**Figure 2.9:** The amplitude of oscillations for  $U < 0$  with  $N_a = 50$

$\coth \frac{N_a \kappa}{2}$  (Eq. (2.37)) quickly approaches 1. We find out that in this limiting case

$$\alpha_1 \rightarrow \frac{1}{4} \frac{2\pi}{N_a} = \frac{\pi}{2N_a} \quad (2.45)$$

just like in the  $U > 0$  case.

The final results for the amplitude of energy oscillations for  $U < 0$  are

$$\Delta E_1 = \Delta E_2 \approx \frac{\sqrt{U^2 + 16}}{8} \frac{\pi^2}{N_a^2} \quad (2.46)$$

As the number of sites increase we observe more pronounced  $\Phi_0/2$  periodicity, which resembles the pairing of electrons as in the superconductivity, but the amplitude of the energy oscillations decrease with inverse square of the number of lattice sites. It is found that, both for the  $U > 0$  and  $U < 0$ , the energy amplitude behaves as  $\frac{1}{N_a^2}$ . But there is a difference between these two cases, the amplitude of oscillations has a dependence on the value of  $U$  for  $U < 0$ , while there is no such dependence for  $U > 0$ .

It can be noted that for  $U < 0$  and  $N_a \gg 1$

$$\cosh \approx \frac{\sqrt{U^2 + 16 \cos^2 \beta}}{4 \cos \beta} \quad (2.47)$$

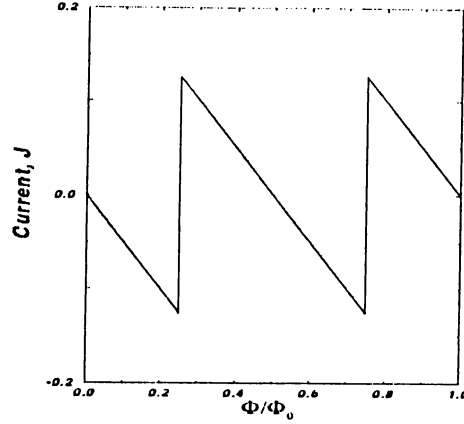


**Figure 2.10:** The current  $J(\Phi)$  for two electrons.

so that,

$$E \approx -\sqrt{U^2 + 16 \cos^2 \beta} \quad (2.48)$$

both for even and odd values of  $n$ .

### The Current $J$

It is possible to write the current as

$$j = -\frac{\partial E}{\partial \phi} \quad (2.49)$$

( $c = 1$  in dimensionless units.) For both  $U > 0$  and  $U < 0$  the behavior of current with large number of sites is as in Fig. (2.10).

First let us consider  $U > 0$ . In Fig. (2.7) we have, for even values of  $n$ ,

$$E = -4 \cos \kappa \cos \left( \frac{Q}{2} + \alpha \right) \quad (2.50)$$

and, for odd value of  $n$ ,

$$E = -4 \cos \frac{\pi}{N_u} \cos \left( \frac{Q}{2} + \alpha \right) \quad (2.51)$$

For these two branches we get the following currents for  $N_a \gg 1$

$$j \approx -4\alpha \quad (2.52)$$

for even  $n$ , and,

$$j \approx -4 \left( \alpha - \frac{\pi}{N_a} \right) \quad (2.53)$$

for odd  $n$ . Hence it is easy to find out that

$$j_m \approx 2 \frac{\pi}{N_a} \quad (2.54)$$

Next we investigate  $U < 0$ . This time we have

$$E = -4 \cosh \kappa \cos \left( \frac{Q}{2} + \alpha \right) \quad (2.55)$$

with  $\kappa$  determined according to the Eqs. (2.49) and (2.50). This time the value of the current depending on  $\alpha$  is as follows

$$j \approx -\sqrt{U^2 + 16} \alpha \quad (2.56)$$

and,

$$j \approx -\sqrt{U^2 + 16} \left( \alpha - \frac{\pi}{N_a} \right) \quad (2.57)$$

so we find out that

$$j_m \approx \frac{\sqrt{U^2 + 16}}{2} \frac{\pi}{N_a} \quad (2.58)$$

The amplitude of the current both for  $U > 0$  and  $U < 0$  has inverse  $N_a$  dependence. As it was in the energy oscillations, the amplitude for large  $N_a$ , has a dependence on  $U$  when  $U$  is attractive, yet, as in the energy oscillations this dependence on  $U$  disappears for positive  $U$ .

## 2.2 Discrete Bethe-Ansatz Equations

The exact solution to 1-d Hubbard model was found by Lieb and Wu<sup>52</sup> in 1968.

The energy eigenvalues are given by

$$E = -2 \sum_{j=1}^{N_e} \cos k_j \quad (2.59)$$

where  $k_j$  are the momenta of the  $N_e$  electrons, which are determined by the discrete Bethe-ansatz equations,<sup>59</sup>

$$\exp(i(k_j - \alpha)N_a) = \prod_{\alpha=1}^M \frac{\sin k_j - \Lambda_\alpha + iU/4}{\sin k_j - \Lambda_\alpha - iU/4} \quad (2.60)$$

$$\prod_{j=1}^{N_e} \frac{\Lambda_\alpha - \sin k_j + iU/4}{\Lambda_\alpha - \sin k_j - iU/4} = - \prod_{\beta=1}^M \frac{\Lambda_\alpha - \Lambda_\beta + iU/2}{\Lambda_\alpha - \Lambda_\beta - iU/2} \quad (2.61)$$

Periodic boundary conditions have been imposed to derive Eqs. (2.61) and (2.62). Here  $\{\Lambda_\alpha\}$  is a set of  $M$  spin repeditics. The  $k$  and  $\Lambda$  values are in general complex numbers.

These equations directly follow from section (2.1) for the case of two electrons with  $M = M' = 1$ , where we derived them using Poisson summation formula. In this section our objective is to trace the dependence of the solution, and therefore the energy  $E$  and the current  $j$ , in the loop for many electrons.

Let us make the following substitutions to simplify these equations,

$$\begin{aligned} \beta &= \frac{Q}{N_e} + \alpha \\ k_j &= \beta + \alpha + x_j, \quad \text{with } \sum_{j=1}^{N_e} x_j = 0 \\ \Lambda_\alpha &= \Lambda + \lambda_\alpha, \quad \text{with } \sum_{\alpha=1}^M \lambda_\alpha = 0 \\ z_j &= \sin k_j - \Lambda \\ u &= U/4 \end{aligned}$$

With the above substitutions, Eqs. (2.61) and (2.62) take the form,

$$\exp(i(k_j - \alpha)N_a) = \prod_{\alpha=1}^M \frac{z_j - \lambda_\alpha + iu}{z_j - \lambda_\alpha - iu} \quad (2.62)$$

$$\prod_{j=1}^{N_e} \frac{-z_j + \lambda_\alpha + iu}{-z_j + \lambda_\alpha - iu} = - \prod_{\beta=1}^M \frac{\lambda_\alpha - \lambda_\beta + 2iu}{\lambda_\alpha - \lambda_\beta - 2iu} \quad (2.63)$$

If we take Eq. (2.64) for all different values of  $\alpha$  ( $\alpha = 1, 2, \dots, M$ ), and multiply them, we get unity. Then, for  $M = M'$ , it follows

$$z_1 = -z_2, \quad z_3 = -z_4, \quad \dots, \quad z_{N_e-1} = -z_{N_e} \quad (2.64)$$

and

$$\lambda_1 = -\lambda_M, \lambda_2 = -\lambda_{M-1} \dots \quad (2.65)$$

if  $M$  is odd  $\lambda_{\frac{M+1}{2}} = 0$ .

These results imply that,

$$\Lambda = \frac{1}{2}(\sin k_1 + \sin k_2) \quad (2.66)$$

and

$$|x_1| = |x_2| = \dots = |x_{N_s}| \quad (2.67)$$

Hence,  $z_1 = z_3 = \dots = -z_2 = -z_4 = \dots = \sin x \cos \beta \equiv z$ . With all of these, Eq. (2.64) for any  $\alpha$  takes the following form,

$$\begin{aligned} \left[ \frac{z - \lambda_\alpha - iu}{z - \lambda_\alpha + iu} \frac{z + \lambda_\alpha + iu}{z + \lambda_\alpha - iu} \right]^M &= - \frac{\lambda_\alpha - \lambda_1 + 2iu}{\lambda_\alpha - \lambda_1 - 2iu} \dots \frac{\lambda_\alpha - \lambda_M + 2iu}{\lambda_\alpha - \lambda_M - 2iu} \\ &= - \prod_{\beta} \frac{\lambda_\alpha - \lambda_\beta + 2iu}{\lambda_\alpha - \lambda_\beta - 2iu} \frac{\lambda_\alpha + \lambda_\beta + 2iu}{\lambda_\alpha + \lambda_\beta - 2iu} \end{aligned} \quad (2.68)$$

From Eq. (2.63), for  $k_j$ 's we get,

$$\begin{aligned} \exp[i(k_1 - \alpha)N_a] &= (-1)^M \exp \left[ -2i \left( \arctan \frac{z - \lambda_1}{u} + \arctan \frac{z - \lambda_2}{u} + \right. \right. \\ &\quad \left. \left. \dots + \arctan \frac{z + \lambda_2}{u} + \arctan \frac{z + \lambda_1}{u} \right) \right] \end{aligned} \quad (2.69)$$

$$\begin{aligned} \exp[i(k_2 - \alpha)N_a] &= (-1)^M \exp \left[ 2i \left( \arctan \frac{z - \lambda_1}{u} + \arctan \frac{z - \lambda_2}{u} + \right. \right. \\ &\quad \left. \left. \dots + \arctan \frac{z + \lambda_2}{u} + \arctan \frac{z + \lambda_1}{u} \right) \right] \end{aligned} \quad (2.70)$$

Note that, it is not necessary to consider all the other  $k_j$ 's, because the equations governing every couple of  $k_{2l+1}$  and  $k_{2l}$  are the same ( $l=1,2, \dots, M-1$ ). Since  $k_1 - k_2 = 2x$ , we have,

$$\frac{x N_a}{2} = \frac{\pi}{2} (I_1 - I_2) - \left( \arctan \frac{z - \lambda_1}{u} + \dots + \arctan \frac{z + \lambda_1}{u} \right) \quad (2.71)$$

where  $I_1$  and  $I_2$  are integers when  $M$  is even, or half-odd integers when  $M$  is odd. We can take the tangent of both sides of the equation(2.72),

$$\tan \frac{x N_a}{2} = \tan \left( \frac{\pi}{2} m - a \right) = -\sigma (\tan a)^\sigma \quad (2.72)$$

$$\text{where } a = \arctan \frac{z - \lambda_1}{u} + \dots + \arctan \frac{z + \lambda_l}{u}$$

Next, we show how the ground state energy is dependent on  $\Phi/\Phi_0$  for some values of  $N_e$ . First of all we start with  $N_e = 2$ . Before, we have found the energy eigenvalue with our formulation. But this time our aim is to arrive at the eigenvalue equation via discrete Bethe-ansatz equations.

### 2.2.1 $N_e = 2$ ( $\uparrow \downarrow$ )

We directly start with the Bethe-ansatz equations for the case of two electrons. We have  $N_e = 2$ ,  $M = M' = 1$ . From equation (2.63) we get,

$$\exp(i(k_1 - \alpha) N_a) = \frac{\sin k_1 - \Lambda + i u}{\sin k_1 - \Lambda - i u} \quad (2.73)$$

$$\exp(i(k_2 - \alpha) N_a) = \frac{\sin k_2 - \Lambda + i u}{\sin k_2 - \Lambda - i u} \quad (2.74)$$

These are the same as Eqs. (2.28) and (2.29), with one exception that  $\Lambda$  is yet unknown. There is only one  $\Lambda_\alpha$ , so we let  $\Lambda_1 = \Lambda$ . Eq. (2.74) and (2.75) take the following simpler forms with the substitutions described on page 43,

$$\exp(i(k_1 - \alpha) N_a) = \frac{z_1 + i u}{z_1 - i u} \quad (2.75)$$

$$\exp(i(k_2 - \alpha) N_a) = \frac{z_2 + i u}{z_2 - i u} \quad (2.76)$$

and,

$$\frac{-z_1 + i u}{-z_1 - i u} \frac{-z_2 + i u}{-z_2 - i u} = 1 \quad (2.77)$$

From this last equation we find out that  $z_1 = -z_2$ . Since  $z_1 = \sin k_1 - \Lambda$  and  $z_2 = \sin k_2 - \Lambda$ , it immediately follows that,

$$\Lambda = \frac{\sin k_1 + \sin k_2}{2} \quad (2.78)$$

As it is easily seen, this result is exactly the same as Eq. (2.25), which was derived with our own formulation.

Next, let us find out the energy eigenvalues  $E = -2(\cos k_1 + \cos k_2)$ . Using Eq. (2.72) we are able to extract all the information we need,

$$\frac{k_1 - k_2}{4} N_a = -\arctan \frac{z}{u} + \frac{\pi}{2} (I_1 - I_2) \quad (2.79)$$

$$\frac{k_1 + k_2}{4} N_a = \alpha N_a + \frac{\pi}{2} (I_1 + I_2) \quad (2.80)$$

Equation (2.80) determines the relation between  $I_1$ ,  $I_2$ , and  $n$ . Hence, the energy eigenvalues of this system are,

$$E = -4 \cos x \cos \beta \quad (2.81)$$

with the following equation for  $x$ ,

$$\tan \frac{N_a x}{2} = -\sigma \left( \frac{\sin x \cos \beta}{u} \right)^\sigma \quad (2.82)$$

with  $\sigma = +1$  for odd values of  $n$ , and  $\sigma = -1$  for even values of  $n$ . So, we finally arrive at the same equations for case of two electrons.

Next we investigate, whether the Bethe-ansatz equations give the extra eigenvalue, which was found in section 2.1. Previously, we have shown that, if two roots were coinciding, the common value of them was one of the possible eigenvalues for the system,

$$E = -4 \cos(Q/2 - K) \cos \beta \quad (2.83)$$

where  $\frac{Q}{2} = \frac{\pi}{N_a} n$ , and  $K = \frac{2\pi}{N_a} n'$ . So the minimum value of  $E$  occurs at the minimum value of  $Q/2 - K$ . Unless  $n$  is even,  $Q/2 - K$  can never be equal to zero, it can at least be  $\frac{\pi}{N_a}$ . Hence, for even values of  $n$  we may have

$$E = -4 \cos \beta \quad (2.84)$$

But observations show that this is not a candidate for minimum energy, since it is not a coinciding root. For odd values of  $n$ ,

$$E = -4 \cos \frac{\pi}{N_a} \cos \beta \quad (2.85)$$

This means that  $x = 0$  and  $x = \frac{\pi}{N_a}$  respectively. For even values of  $n$ , this energy value is higher than other possible eigenvalues, hence it can not be a candidate for the ground state energy. When we investigate the Bethe-ansatz equations carefully, we find out that  $x = \frac{\pi}{N_a}$  is not a solution. Moreover, the equations give  $x = 0$  for odd values of  $n$ , which actually is impossible (for  $U > 0$ , it is clear that  $E^2 < E_0^2$ , hence  $E$  is always larger than  $-4 \cos \beta$ ).

During our literature search, we have found several mistakes in certain papers. For example, starting directly from Bethe-ansatz equations, Kusmartsev et. al.<sup>21</sup> have arrived at erroneous results. The main mistake is, of course, these equations do not give the extra eigenvalues that we have found, and the equations also cover  $x = 0$ , which should actually be excluded. Furthermore, people start from Eq. (9) and Eq. (10) of Lieb and Wu's paper<sup>52</sup> and consider the integers ( $I_1$  and  $I_2$ ) there as independent from each other. Actually, if the calculations are carried out from the very beginning, it is seen that these integers have dependencies on each other. So we conclude that there are some extra eigenvalues which can never be obtained by Bethe-ansatz equations. Besides, some eigenvalues given by the same equations are incorrect.

### 2.2.2 $N_e = 4$ ( $\uparrow \uparrow \downarrow \downarrow$ )

If we start directly from Eq. (2.44), we get,

$$\left[ \frac{z^2 - (\lambda + iu)^2}{z^2 - (\lambda - iu)^2} \right]^2 = \frac{\lambda + iu}{\lambda - iu} \quad (2.86)$$

The value of  $\lambda$  can be calculated from the above equation,

$$\lambda^2 = \frac{z^2 - u^2}{3} \pm \frac{2}{3} \sqrt{u^4 + u^2 z^2 + z^4} \quad (2.87)$$

From Eq. (2.70) and Eq. (2.71),

$$(k_1 - \alpha)N_a = -2 \left( \arctan \frac{z - \lambda}{u} + \arctan \frac{z + \lambda}{u} \right) + 2\pi n_1 \quad (2.88)$$

and,

$$(k_2 - \alpha)N_a = 2 \left( \arctan \frac{z - \lambda}{u} + \arctan \frac{z + \lambda}{u} \right) + 2\pi n_2 \quad (2.89)$$

So,  $(k_1 + k_2)N_a = 2\alpha N_a + 2\pi(n_1 + n_2)$ , which means  $n_1 + n_2 = n$ , where  $n$  is the integer in the  $Q = \frac{2\pi}{N_a} n$ . The eigenvalue equation is,

$$E = -8 \cos x \cos \beta \quad (2.90)$$

with  $x$  determined by the equation,

$$\tan \frac{x N_a}{2} = -\sigma \left( \frac{2u \sin x \cos \beta}{u^2 - \sin^2 x \cos^2 \beta + \lambda^2} \right)^\sigma \quad (2.91)$$

with  $\sigma = +1$  if  $n$  is even, otherwise  $\sigma = -1$ .

### 2.2.3 $N_e = 6, 8, 10, \dots$

For  $N_e = 6$  ( $M = 3$ ) we have,

$$\frac{x N_a}{2} = \frac{\pi}{2} m - \left( \arctan \frac{z - \lambda}{u} + \arctan \frac{z}{u} + \arctan \frac{z + \lambda}{u} \right) \quad (2.92)$$

with  $\lambda$  determined by,

$$\left[ \frac{z^2 - (\lambda + iu)^2}{z^2 - (\lambda - iu)^2} \right]^3 = \frac{\lambda + iu}{\lambda - iu} \frac{\lambda + 2iu}{\lambda - 2iu} \quad (2.93)$$

and  $m$  is odd if  $n$  is even, it is even if  $n$  is odd

For  $N_e = 8$  ( $M = 4$ ) we have,

$$\begin{aligned} \frac{x N_a}{2} = \frac{\pi}{2} m - \left( \arctan \frac{z - \lambda_1}{u} + \arctan \frac{z - \lambda_2}{u} \right. \\ \left. + \arctan \frac{z + \lambda_2}{u} + \arctan \frac{z + \lambda_1}{u} \right) \end{aligned} \quad (2.94)$$

where  $m$  is even if  $n$  is even, odd if  $n$  is odd. Also,  $\lambda_1$  and  $\lambda_2$  are determined by,

$$\left[ \frac{z^2 - (\lambda_1 + iu)^2}{z^2 - (\lambda_1 - iu)^2} \right]^4 = \frac{\lambda_1 - \lambda_2 + 2iu}{\lambda_1 - \lambda_2 - 2iu} \frac{\lambda_1 + \lambda_2 + 2iu}{\lambda_1 + \lambda_2 - 2iu} \frac{\lambda_1 + iu}{\lambda_1 - iu} \quad (2.95)$$

and

$$\left[ \frac{z^2 - (\lambda_2 + iu)^2}{z^2 - (\lambda_2 - iu)^2} \right]^4 = \frac{\lambda_2 - \lambda_1 + 2iu}{\lambda_2 - \lambda_1 - 2iu} \frac{\lambda_2 + \lambda_1 + 2iu}{\lambda_2 + \lambda_1 - 2iu} \frac{\lambda_2 + iu}{\lambda_2 - iu} \quad (2.96)$$

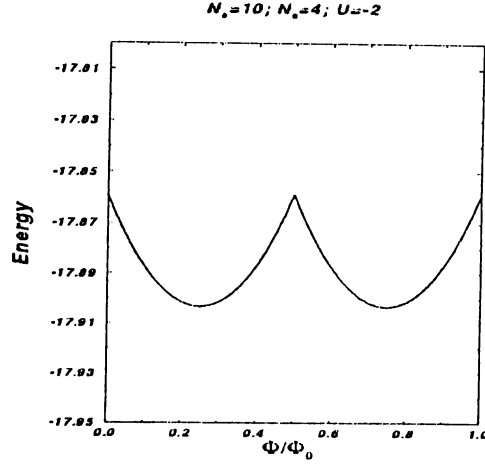


**Figure 2.11:** The dependence of energy on the flux for  $N_c = 4$ .

And the equations go on like this for  $M > 4$ . We can summarize the result as follows:

i) If  $M$  is odd,  $M = 2l + 1$ ,

$$\tan \frac{x N_a}{2} = -\sigma (\tan a)^\sigma \quad (2.97)$$

where,

$$a = \arctan \frac{z - \lambda_1}{u} + \dots + \arctan \frac{z - \lambda_l}{u} + \arctan \frac{z + \lambda_l}{u} + \dots + \arctan \frac{z + \lambda_1}{u} \quad (2.98)$$

with,

$$\sigma = \begin{cases} +1 & \text{if } n \text{ is odd} \\ -1 & \text{if } n \text{ is even} \end{cases} \quad (2.99)$$

Where the  $\lambda$ 's are determined from Eq. (2.69).

ii) If  $M$  is even,  $M = 2l$ ,

$$\tan \frac{x N_a}{2} = -\sigma (\tan a)^\sigma \quad (2.100)$$

where,

$$a = \arctan \frac{z - \lambda_1}{u} + \cdots + \arctan \frac{\lambda_l}{u} + \arctan \frac{+ \lambda_l}{u} + \cdots + \arctan \frac{z + \lambda_1}{u} \quad (2.101)$$

with,

$$\sigma = \begin{cases} +1 & \text{if } n \text{ is even} \\ -1 & \text{if } n \text{ is odd} \end{cases} \quad (2.102)$$

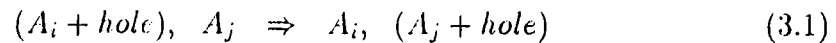
Where the  $\lambda$ 's are determined from Eq. (2.69).

## Chapter 3

# CONTRACTION MODEL

In the introduction chapter we have described the idea of the intrinsic-hole metal as opposed to the conventional, intrinsic-electron metals, and introduced the new type of hole interaction called the 'contraction interaction'.

Intrinsic holes are not totally equivalent to the intrinsic electrons in the sense that they can not be fully removed from the parent atom. But the external atoms can provide a proper surrounding in which the hole may reside. The important thing is the possibility of hole hopping between different sites  $(i, j)$



The difference between 'intrinsic-electron' and 'intrinsic-hole' type metals is illustrated in Fig. (3.1).

Normally two oxygen atoms have strong tendency to make covalent bonding, resulting in the formation of oxygen molecule,  $O_2$ . However in a proper chemical surrounding, this may not happen if the nearest neighbor atoms are not too close to each other. In such a case, the other scenario will apply, reminiscent of metallic oxygen. We may suppose that this is just what happens in the metal-oxide superconductors. In the  $CuO_2$  plane of the latter, due to large ionic radii of copper, oxygen orbitals overlap between themselves almost as strongly as the near site oxygen and copper orbitals. Then the  $O_2$  molecules are not formed, and the electrons derived from the  $p^6$  shell are to conduct. The charge carriers are

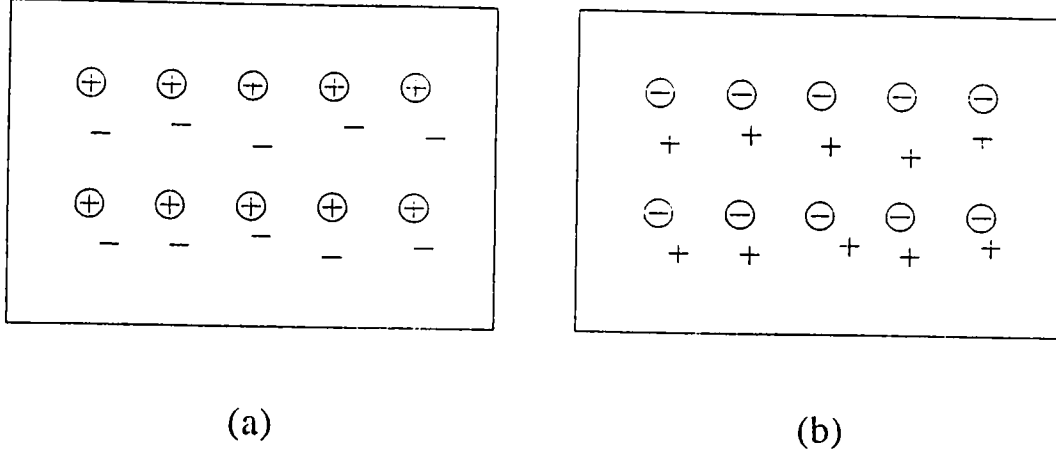


**Figure 3.1:** Intrinsic-electron and intrinsic-hole type metals. (a) Cation network with the intrinsic electrons condensing to a Fermi liquid. (b) The anion network with intrinsic holes as a Fermi liquid of positive charge.

holes in the  $p^6$  shell, propagating from one oxygen anion to the next nearest one by hopping.

As we have discussed before, the Hamiltonian for the contraction model is

$$\begin{aligned}
 H = & - \sum_{i,\sigma} c_{i,\sigma}^\dagger c_{i+1,\sigma} \exp(i\alpha) + h.c. + U \sum_i n_{i,\uparrow} n_{i,\downarrow} \\
 & + \sum_{i,\sigma} c_{i,\sigma}^\dagger c_{i+1,\sigma} [V n_{i,-\sigma} n_{i+1,-\sigma} + W(n_{i,-\sigma} + n_{i+1,-\sigma})] \exp(i\alpha) + h.c. \quad (3.2)
 \end{aligned}$$

### 3.1 Bound States of Two Electrons

As in section 2.1 the wave function for two electrons, one with spin up the other with spin down, can be described as:

$$|\Psi\rangle = \sum_{x_1, x_2} f(x_1, x_2) c_{x_1, \uparrow}^\dagger c_{x_2, \downarrow}^\dagger |0\rangle \quad (3.3)$$

The eigenvalue equation  $H|\Psi\rangle = E|\Psi\rangle$  leads to

$$\begin{aligned}
& -[(f(x_1 + 1, x_2) + f(x_1, x_2 + 1)) \exp(i\alpha) \\
& \quad + (f(x_1 - 1, x_2) + f(x_1, x_2 - 1)) \exp(-i\alpha)] \\
& + U\delta(x_1, x_2)f(x_1, x_2) \\
& + W\{[f(x_1 + 1, x_2)(\delta(x_1, x_2) + \delta(x_1 + 1, x_2)) \\
& \quad + f(x_1, x_2 + 1)(\delta(x_1, x_2) + \delta(x_1, x_2 + 1))] \exp(i\alpha) \\
& \quad + [f(x_1 - 1, x_2)(\delta(x_1, x_2) + \delta(x_1 - 1, x_2)) \\
& \quad + f(x_1, x_2 - 1)(\delta(x_1, x_2) + \delta(x_1, x_2 - 1))] \exp(-i\alpha)\} \\
& = Ef(x_1, x_2)
\end{aligned} \tag{3.4}$$

Changing from coordinate representation to the Fourier representation (see Eqs. (2.7) and (2.8)), we obtain

$$\begin{aligned}
& (E + 2 \cos(K_1 + \alpha) + 2 \cos(K_2 + \alpha))f_{K_1, K_2} = \frac{U}{N_a} \sum_K f_{K_1 - K, K_2 + K} \\
& + \frac{W}{N_a} \sum_K 2 (\cos(K_1 + \alpha) + \cos(K_2 + \alpha) + \cos(K_1 - K + \alpha) + \cos(K_2 + K + \alpha)) \times \\
& \quad \times f_{K_1 - K, K_2 + K}
\end{aligned} \tag{3.5}$$

Letting  $\varepsilon_k = 2 \cos k$ , we get

$$\begin{aligned}
& f_{K_1, K_2} = \\
& \frac{\frac{U}{N_a} \sum_K f_{K_1 - K, K_2 + K} + \frac{W}{N_a} \sum_K (\varepsilon_{K_1 + \alpha} + \varepsilon_{K_2 + \alpha} + \varepsilon_{K_1 - K + \alpha} + \varepsilon_{K_2 + K + \alpha}) f_{K_1 - K, K_2 + K}}{E + (\varepsilon_{K_1 + \alpha} + \varepsilon_{K_2 + \alpha})}
\end{aligned} \tag{3.6}$$

For a short hand notation, let us make the following definitions

$$\frac{1}{N_a} \sum_K f_{K_1 - K, K_2 + K} \equiv F_0(Q) \tag{3.7}$$

and,

$$\frac{1}{N_a} \sum_K (\varepsilon_{K_1 - K + \alpha} + \varepsilon_{K_2 + K + \alpha}) f_{K_1 - K, K_2 + K} \equiv F_1(Q) \tag{3.8}$$

which are functions of only  $Q = K_1 + K_2$  in mod  $2\pi$ . After a second summation Eq.(3.6) becomes

$$\begin{aligned}
F_0(Q) &= F_0(Q) \frac{U}{N_a} \sum_p \frac{1}{E + (\varepsilon_{K_1-\rho+\alpha} + \varepsilon_{K_2+\rho+\alpha})} \\
&+ F_0(Q) \frac{W}{N_a} \sum_p \frac{\varepsilon_{K_1-\rho+\alpha} + \varepsilon_{K_2+\rho+\alpha}}{E + (\varepsilon_{K_1-\rho+\alpha} + \varepsilon_{K_2+\rho+\alpha})} \\
&+ F_1(Q) \frac{W}{N_a} \sum_p \frac{1}{E + (\varepsilon_{K_1-\rho+\alpha} + \varepsilon_{K_2+\rho+\alpha})}
\end{aligned} \tag{3.9}$$

and with multiplication by  $\varepsilon_{K_1-\rho+\alpha} + \varepsilon_{K_2+\rho+\alpha}$  followed by a summation over  $p$

$$\begin{aligned}
F_1(Q) &= F_0(Q) \frac{U}{N_a} \sum_p \frac{\varepsilon_{K_1-\rho+\alpha} + \varepsilon_{K_2+\rho+\alpha}}{E + (\varepsilon_{K_1-\rho+\alpha} + \varepsilon_{K_2+\rho+\alpha})} \\
&+ F_0(Q) \frac{W}{N_a} \sum_p \frac{(\varepsilon_{K_1-\rho+\alpha} + \varepsilon_{K_2+\rho+\alpha})^2}{E + (\varepsilon_{K_1-\rho+\alpha} + \varepsilon_{K_2+\rho+\alpha})} \\
&+ F_1(Q) \frac{W}{N_a} \sum_p \frac{\varepsilon_{K_1-\rho+\alpha} + \varepsilon_{K_2+\rho+\alpha}}{E + (\varepsilon_{K_1-\rho+\alpha} + \varepsilon_{K_2+\rho+\alpha})}
\end{aligned} \tag{3.10}$$

Letting

$$\frac{1}{N_a} \sum_p \frac{1}{E + (\varepsilon_{K_1-\rho+\alpha} + \varepsilon_{K_2+\rho+\alpha})} \equiv S_0(E) \tag{3.11}$$

and,

$$\frac{1}{N_a} \sum_p \frac{\varepsilon_{K_1-\rho+\alpha} + \varepsilon_{K_2+\rho+\alpha}}{E + (\varepsilon_{K_1-\rho+\alpha} + \varepsilon_{K_2+\rho+\alpha})} \equiv S_1(E) \tag{3.12}$$

and,

$$\frac{1}{N_a} \sum_p \frac{(\varepsilon_{K_1-\rho+\alpha} + \varepsilon_{K_2+\rho+\alpha})^2}{E + (\varepsilon_{K_1-\rho+\alpha} + \varepsilon_{K_2+\rho+\alpha})} \equiv S_2(E) \tag{3.13}$$

Eqs. (3.9) and (3.10) can be written in the following form:

$$F_0(Q) = U F_0(Q) S_0(E) + W F_0(Q) S_1(E) + W F_1(Q) S_0(E) \tag{3.14}$$

and,

$$F_1(Q) = U F_0(Q) S_1(E) + W F_0(Q) S_2(E) + W F_1(Q) S_1(E) \tag{3.15}$$

In the matrix form

$$\begin{vmatrix} 1 - U S_0(E) - W S_1(E) & -W S_0(E) \\ U S_1(E) + W S_2(E) & -1 + W S_1(E) \end{vmatrix} = 0 \tag{3.16}$$

or,

$$F_0(E) = F_1(E) = 0 \quad (3.17)$$

The second solution, Eq. (3.17), is possible only if the requirement, that two roots coincide, which was presented in section (2.1), is fulfilled. In this case the energy eigenvalue of the system becomes

$$E = -2 \cos(K_1 + \alpha) - 2 \cos(K_2 + \alpha) \quad (3.18)$$

Observing the fact that,

$$\begin{aligned} S_1(E) &= \frac{1}{N_a} \sum_p \frac{\varepsilon_{K_1-p+\alpha} + \varepsilon_{K_2+p+\alpha}}{E + (\varepsilon_{K_1-p+\alpha} + \varepsilon_{K_2+p+\alpha})} \\ &= \frac{1}{N_a} \sum_p \frac{E + (\varepsilon_{K_1-p+\alpha} + \varepsilon_{K_2+p+\alpha})}{E + (\varepsilon_{K_1-p+\alpha} + \varepsilon_{K_2+p+\alpha})} - \frac{E}{N_a} \sum_p \frac{1}{E + (\varepsilon_{K_1-p+\alpha} + \varepsilon_{K_2+p+\alpha})} \\ &= 1 - ES_0(E) \end{aligned} \quad (3.19)$$

and with a similar procedure,

$$S_2(E) = -E + E^2 S_0(E) \quad (3.20)$$

From Eq. (3.16), the transcendental equation is found as follows

$$\frac{(W-1)^2}{U+W(W-2)E} = S_0(E) \quad (3.21)$$

The plot of this transcendental equation is presented in Fig.(3.2). Equation (3.21) can be solved numerically and the value of the energy  $E$  can be found. If we set  $W = 0$  in this final equation, we immediately get the result in 1-d Hubbard Model (see Eq. (2.14)). The points where  $S_0(E)$  intersects with the LHS, are the eigenvalues  $E$  of the system (see Fig. (3.3)). In these solutions  $W$  has great importance. The effect of it can be summarized as follows:

(i) Minimum energy is found by  $\frac{(W-1)^2}{U+W(W-2)E} = S_0(E)$  for all even  $n$ . But if  $n$  is odd this equation is adequate for minimum energy in the case when

$$W(W-2) > 0 \text{ and } E_{cr} > E_0 \quad (3.22)$$

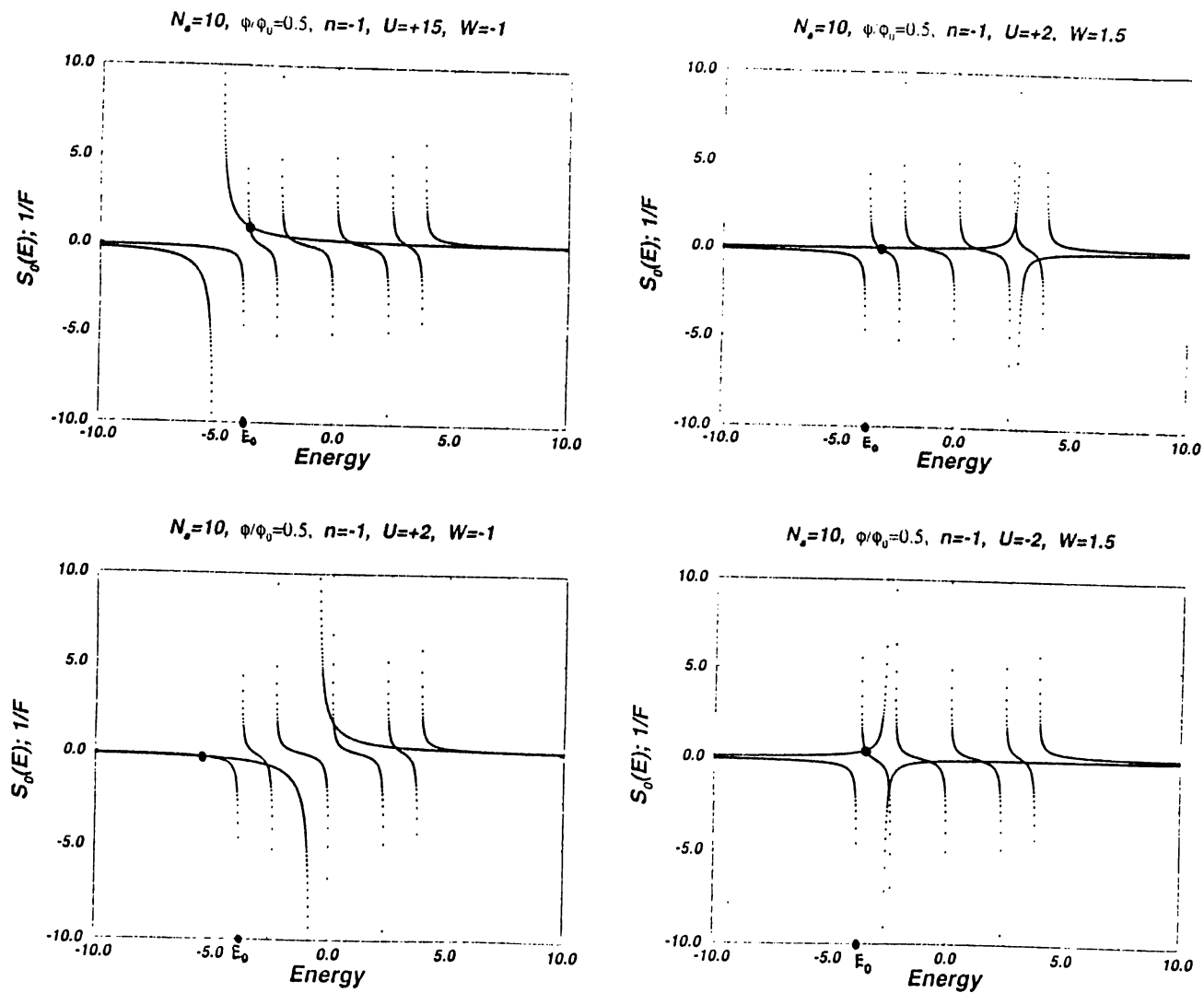


**Figure 3.2:** Plot of the transcendental equation for the contraction model  
 In contrast to 1-d Hubbard model, there may be bound states with energies less than  $E_0$  for positive  $U$ , with an appropriate value of  $W$ . On the other hand, for  $U < 0$ , and some values of  $W$ , eigenvalue  $E$  can never be smaller than  $E_0$ , that is  $E^2 < E_0^2$ .

or

$$W(W - 2) < 0 \text{ and } E_{cr} < E_0 \quad (3.23)$$

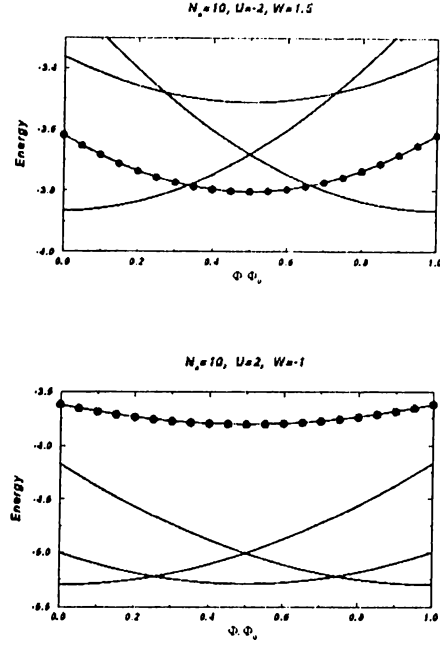


**Figure 3.3:** Energy versus flux for two electrons in the contraction mechanism. The straight lines corresponds to Eq. (3.21), the dotted one corresponds to Eq. (3.18).

where

$$E_{cr} = -\frac{U}{W(W-2)}, \quad E_0 = -4 \cos(Q/2 - K) \cos(Q/2 + \alpha) \quad (3.24)$$

(ii) Minimum energy can be  $E = E_0$  when  $n$  is odd and the following conditions are satisfied,

$$W(W-2) > 0 \text{ and } E_{cr} < E_0 \quad (3.25)$$

or

$$W(W-2) < 0 \text{ and } E_{cr} > E_0 \quad (3.26)$$

With the similar calculations (from Eq. (3.21)) as in section (2.1), we get the following result

$$\exp(ik_1 N_a) \exp(-i\alpha) = \frac{\sin k_1 - \Lambda + iF/4}{\sin k_1 - \Lambda - iF/4} \quad (3.27)$$

and,

$$\exp(ik_2 N_a) \exp(-i\alpha) = \frac{\sin k_2 - \Lambda + iF/4}{\sin k_2 - \Lambda - iF/4} \quad (3.28)$$

where,

$$F = \frac{U + W(W - 2)E}{(W - 1)^2} \quad (3.29)$$

and as before,

$$\Lambda = \frac{\sin k_1 + \sin k_2}{2} \quad (3.30)$$

Also as before the momenta of the two electrons are

$$k_1 = \frac{Q}{2} + \alpha + x$$

$$k_2 = \frac{Q}{2} + \alpha - x$$

where

$$x = \begin{cases} \kappa & \text{if } E^2 < E_0^2 \\ i\kappa & \text{if } E^2 > E_0^2 \end{cases} \quad (3.31)$$

Hence the eigenvalue equation is

$$E = -4 \cos x \cos \beta \quad (3.32)$$

with  $x$  determined by

$$\tan \frac{N_a x}{2} = -\sigma \left( \frac{4(W - 1)^2 \sin x \cos \beta}{U - 4W(W - 2) \cos x \cos \beta} \right)^\sigma \quad (3.33)$$

and  $\sigma = +1$  for odd value and  $\sigma = -1$  for even value of  $n$ .

## 3.2 The Overlap Integral

To have an idea about the occupation dependent hopping, we investigate the anion network in the  $CuO_2$  plane as in Fig. (3.4). The hopping integral between oxygens is

$$t = \int \Psi_1^*(\vec{r}) (V(\vec{r}) - V_a(\vec{r})) \Psi_2(\vec{r}) dV \quad (3.34)$$

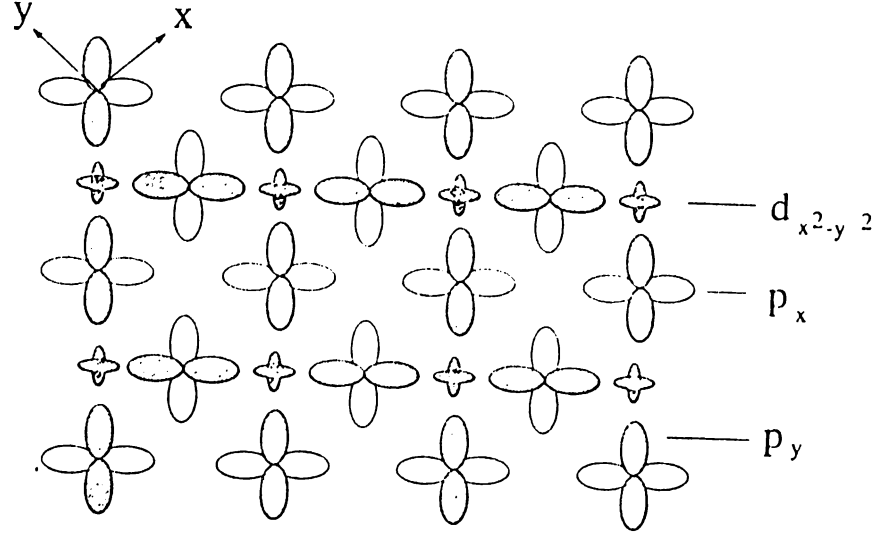


Figure 3.4: The  $CuO_2$  network.

The functions,  $\Psi_1$  and  $\Psi_2$  are very rapidly decaying with increasing  $r$ . While,  $V(\vec{r}) - V_a(\vec{r})$  is a rather slow one. Hence, we can approximately write,

$$t \approx I_{12} = \vec{V} \int \Psi_1^*(\vec{r}) \Psi_2(\vec{r}) dV \quad (3.35)$$

where

$$\Psi_{1,2}(r_{1,2}) = \sin \theta_{1,2} \cos \phi_{1,2} R(r_{1,2}) \quad (3.36)$$

A proper reference can be the one in Fig.(3.4). In this reference frame we write the above wave functions in terms of new coordinates. After some geometrical transformations, the wave functions take the following forms

$$\Psi_1 = \sqrt{\frac{3}{8\pi}} \sin \theta (\cos \phi - \sin \phi) R(r) \quad (3.37)$$

and,

$$\Psi_2 = \sqrt{\frac{3}{8\pi}} \frac{r \sin \theta (\cos \phi + \sin \phi) + a}{\rho} R(\rho) \quad (3.38)$$

where

$$\rho = \sqrt{r^2 + 2ar \sin \theta \sin \phi + a^2} \quad (3.39)$$

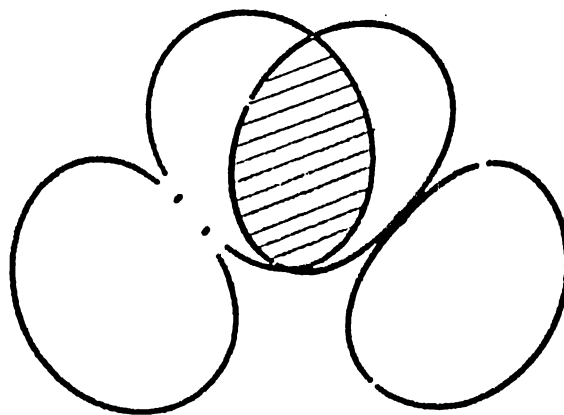


**Figure 3.5:** Overlapping orbitals of the oxygen atoms.

and  $a$  is the spacing between the oxygen atoms (see Fig. (3.5)).

Next we numerically calculate the overlap integral  $I_{12}$ . We calculate the integral as follows,

$$\int_V \Psi_1 \Psi_2 dV \rightarrow \sum_i \sum_j \sum_k \Psi_1(r_i, \theta_j, \phi_k) \Psi_2(r_i, \theta_j, \phi_k) r_i^2 \Delta r \sin \theta_j \Delta \theta \Delta \phi \quad (3.40)$$

We calculate the integrals for the following  $O$  atoms

$$t_0: O_i^- + O_j^{2-} \Rightarrow O_i^{2-} + O_j^-$$

$$t_1: O_i + O_j^{2-} \Rightarrow O_i^{2-} + O_j$$

$$t_2: O_i + O_j^- \Rightarrow O_i^- + O_j$$

We use the Herman-Skilman<sup>44</sup> program to determine the radial parts of the wave functions. But this program is not very suitable for negative ions, and does not give very precise results, especially for the  $O^{2-}$  case. We believe that if it was possible to find a better computer program or a better procedure, the overlap integrals corresponding to  $t_0$  and  $t_1$  would be greater. The results of the integrations are discussed in the following section.

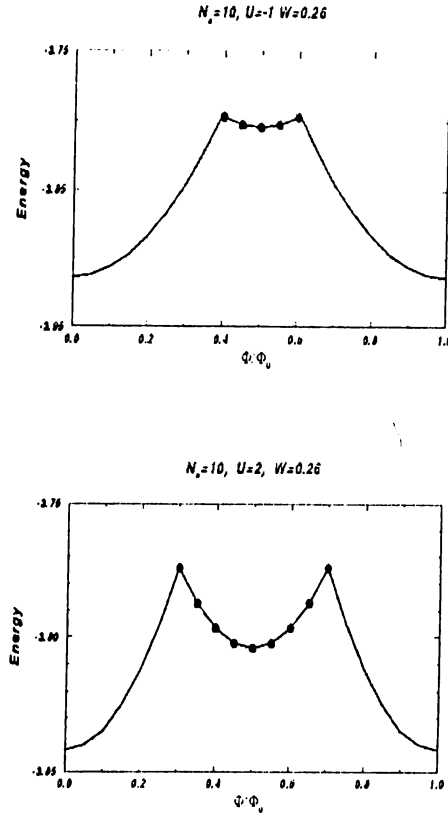


Figure 3.6: Energy versus flux with the results of overlap integration.

### 3.2.1 Interpretation of the Results

We found that  $t_0 = 0.222$  and  $t_1 = 0.161$ . With the definitions (Eq. (1.34))

$$t = -t_0 = -0.222 \quad (3.11)$$

and,

$$W = t_1 - t_0 = -0.058 \quad (3.12)$$

If we let  $t = 1$  then  $W = 0.26$ . That is,  $W$  is in the range  $[0, 2]$ . In this region, to have bound states,  $E_{cr}$  should be smaller than  $E_0$ . For positive  $U$ ,  $E_{cr}$  is always larger than 0, hence  $E_{cr} > E_0$ . In the case of negative  $U$  both are possible.

Depending on the value of  $U$ ,  $E_{cr}$  may either be larger or smaller than  $E_0$ .

With this value of  $W$ , we do not get much new thing for  $U > 0$ . We still have no period halving for the situation when Eq. (3.17) is not taken into account (just as in the 1-d Hubbard model). But for  $U < 0$ , we get a totally different picture. For some values of negative  $U$ , the ground state energy of the system becomes larger, and a periodic behavior, which is similar to the one for 1-d Hubbard model with  $U > 0$  appears.

# Chapter 4

## CONCLUSION

We have studied the strongly correlated models of electron systems. The major objective was to search for a mechanism of high  $T_c$  superconductivity. The other objective was to see the effect of quantum phenomena in mesoscopic structures. The key method for the possibility of superconductivity is to look at the flux dependence of the energy and the amplitude of the nondecaying current. This current is nominated as persistent current in small systems and supercurrent in larger systems. We have worked on Hubbard model with attractive interaction, Hubbard model with repulsive interaction and contraction model, which takes the occupation at the sites into account.

In case of Hubbard model, by using the Poisson summation method, we derived the Bethe-ansatz equations for attractive and repulsive interaction for two electrons with a magnetic flux  $\Phi$  applied. For  $\Phi = 0$  our results have reduced to the Bethe-ansatz equations. However, we have found that Bethe-ansatz equations give incomplete solutions.

We have found that the oscillation of the energy has amplitude proportional to inverse square of  $N_a$  for repulsive  $U$ . But it was not a supercurrent, it was rather a behavior do to the mesoscopic nature of the system. For attractive  $U$  the amplitude of oscillations are much larger than the repulsive  $U$  case. When strong electron interactions are considered,  $|U/t|$  becomes larger and the amplitude of oscillations depend on this value. We have also found the flux dependence of

energy for the model with more than two electrons.

We found the analytical solution to contraction mechanism for two electrons. The solutions do not depend on  $V$ , however they heavily depend on  $W$ . In contrast to 1-d Hubbard model, there may be bound states with energies less than  $E_0$  for positive  $U$  (intersection points to the left of  $E_0$  in Fig. (3.2)), with an appropriate value of  $W$ . Still unlike the 1-d Hubbard Model, for  $U < 0$ , and some certain values of  $W$ ,  $E^2$  is always smaller than  $E_0^2$  (in 1-d Hubbard model, for  $U < 0$ ,  $E^2$  was always larger than  $E_0^2$ ).

We performed some numerical calculations, to get an intuitive idea for the values of  $t$  and  $W$ . With the calculated values of  $W$  and  $t$ , we did not get much new thing for  $U > 0$ . We still have no period halving unless Eq. (3.17) is taken into account (just as in the 1-d Hubbard model). But for  $U < 0$ , we got a completely different behavior. For small absolute values of negative  $U$ , the ground state energy of the system becomes larger, and a periodic behavior, which shows similar characteristics as the 1-d Hubbard model with  $U > 0$  appears, that is period halving appears only if the solution corresponding to Eq. (3.17) is taken into account.

# Bibliography

- [1] Y. Imry and D. J. Bergman, Phys. Rev. **A3**, 1416 (1971)
- [2] M. E. Fisher In: *Proceedings of the International Summer School Enrico Fermi*, Varenna, Italy, Course 51, M. S. Green, ed.(Academic Press, New York), (1971).
- [3] J. E. Hirsch, Phys. Lett. A **134**, 451, (1989).
- [4] S. Washburn In: *Mesoscopic Phenomena in Solids*, p.3 Eds. B. L. Al'tshuler, P. A. Lee and R. A. Webb. North-Holland, (1991).
- [5] H. Heinrich, G. Bauer and F. Kuchar, editors, *Physics and Technology of Submicron Devices*, Springer, Berlin (1988).
- [6] R. A. Webb and R. B. Laibowitz, editors, special issue on: '*Mesoscopic phenomena and nanolithographic technology*', IBM Journal of Research and Development, **32** (No:3-4), (1988)
- [7] T. T. Wu and C. N. Yang, Physical Review D **12**, 3845, (1975).
- [8] M. A. Reed and W. P. Kirk, editors, *Nanostructure Physics and Fabrication*, Academic Press, New York, (1989).
- [9] P. A. Lee, R. A. Webb and B. L. Al'tshuler, editors, *Mesoscopic Phenomena in Solids*, Elsevier, Amsterdam, (1989).
- [10] N. M. Plakida, *High-Temperature Superconductors* Springer-Verlag, (1993).

- [11] R. Landauer, *Phil. Mag.* **21**, 863 (1970).
- [12] R. Laibowitz In: *Percolation, Localization and Superconductivity*, A. M. Goldman and S. A. Wolf, eds., NATO Advanced Science Institutes, Series B: Physics, 109 (Plenum, New York)
- [13] M. Ya Azbel, *Solid State Commun.* **45**, 527 (1983).
- [14] P. W. Anderson, *Science* **235**, 1196, (1987). J. M. Wheatley, T. C. Hsu, and P. W. Anderson, *Physical Review B* **37**, 5897, (1988).
- [15] M. Ya Azbel, *Physical Review Letters* **31**, 589 (1973).
- [16] P. W. Anderson, D. J. Thouless, E. Abrahams, D. S. Fisher, *Physical Review* **B22**, 3519 (1980)
- [17] Y. Gefen, Y. Imry, M. Ya Azbel, *Physical Review Letters* **52**, 129 (1984).
- [18] Y. Gefen, Y. Imry, M. Ya Azbel, *Surf. Sci.* **142** (1984).
- [19] A. B. Fowler, U. S. Patent 4550330 (1985).
- [20] S. Datta, M. Melloch, S. Bandyopadhyay, S. Lundstromm, *Appl. Phys. Lett.* **48**, 487, (1986).
- [21] F. V. Kusmartsev, J. F. Weisz and R. Kishore, Minoru Takahashi, *Strong Correlations Versus U-center Pairing and Fractional Aharanov-Bohm Effect*, *Physical Review B* **49**, 16 234 (1994).
- [22] I. O. Kulik, *Flux Quantization in a Normal Metal*, *JETP Lett.* **11**, 275 (1970).
- [23] W. Ehrenberg and R. W. Siday, *Proc. Phys. Soc. London* **B62**, 8, (1949).
- [24] Y. Aharonov and D. Bohm, *Significance of Electromagnetic Potentials in the Quantum Theory*, *Physical Review* **115**, 485, (1959)
- [25] Y. Aharonov and D. Bohm, *Physical Review* **123**, 1511, (1961).

- [26] W. H. Furry and N. F. Ramsey, Phys. Rev. **118**, 426, (1960).
- [27] G. Mollenstedt and W. Bayh, Phys. Blatter **18**, 299, (1962); Naturwiss. **4**, 81, (1962).
- [28] B. S. DeWitt, Phys. Rev. **125**, 2189, (1962).
- [29] M. Peshkin, I. Talmi, and L. J. Tassie, Ann. Phys. **16**, 426, (1960).
- [30] R. G. Chambers, Phys. Rev. Lett. **5**, 3, (1960).
- [31] K. B. Lyons, P. A. Fleury, J. P. Remoike, and T. J. Negran, Physical Review B **37**, 2353, (1988). K. B. Lyons, P. A. Fleury, J. P. Remoike, A. S. Cooper, and T. J. Negran, Physical Review B **37**, 2353. (1988).
- [32] L. J. Tassie, Physics Letters **5**, 43, (1963).
- [33] B. L. Al'tshuler, A. G. Aronov, B. Z. Spivak, D. Yu. Sharvin, and Yu. V. Sharvin, *Observation of Aharonov-Bohm effect in hollow metal cylinders*, JETP Letters **35**, 588, (1982)
- [34] B. L. Al'tshuler, A. G. Aronov, and B. Z. Spivak. *The Aharonov-Bohm effect in disordered conductors*, JETP Letters **33**, 94, (1981).
- [35] J. Bardeen, L. N. Cooper, and J. R. Schrieffer, Physical Review **108**, 1175, (1957).
- [36] J. R. Bednorz and K. A. Müller, Z. Phys. B **64**, 189, (1986). For more information concerning high  $T_c$  superconductivity, see for instance: H. Ehrenreich and D. Turnbull (eds.) (Academic Press, New York, 1989), **42**. J. C. Phillips, *Physics of High  $T_c$  Superconductivity* (Academic Press, New York, 1989). J. W. Lynn (ed.) *High Temperature Superconductivity* (Springer-Verlag, New York, 1990). D. M. Ginsberg (ed.), *Physical Properties of High Temperature Superconductors* (World Scientific, Teaneck, NJ, 1989, 1990).
- [37] Timothy H. Boyer, *Misinterpretation of the Aharonov-Bohm Effect*, AJP **40** 56, (1972).

- [38] M. Buttiker, Y. Imry and R. Landauer, Phys. Lett. **96A**, 365 (1983)
- [39] V.Chandrasekhar, Q. A. Webb, M. J. Brady et al., Physical Review Letters **67**, 3578 (1991)
- [40] G. M. Eliashberg, Zh. Eksp. Teor. Fiz. **38**, 966, (1960) [Sov. Phys.-JETP **11**, 696, (1960)]; **43**, 1005, (1962) [**16**, 780, (1963)]. D. J. Scalapino, J. R. Schrieffer, and J. W. Wilkins, Phys. Rev. **148**, 263, (1966).
- [41] V. J. Emery and G. Reiter, Phys. Rev. B **38**, 4547, (1988).
- [42] A. B. Fowler, U. S. Patent 4550330 (1985).
- [43] H. D. Hahlbohm and H. Lübbig, eds. *Proceedings of the Third International Conference on Superconducting Quantum Devices*, Berlin, (de Gruyter, Berlin) contains recent references (1985).
- [44] Frank Herman and Sherwood Skillman, *Atomic Structure Calculations*, Prentice-Hall, Inc., (1963).
- [45] J. E. Hirsch, Phys. Lett. A **134**, 451, (1989).
- [46] Y. Imry, Phys. Rev. **B15**,4478 (1977)
- [47] I. O. Kulik, In: *Seminars on Mesoscopic Physics, Bilkent University Department of Physics*, (1993).
- [48] I. O. Kulik, *Contraction Mechanism for Pairing Interaction in Oxides and Hydrides*, in: Progress in High Temperature Physics, vol. 25, ed. R. Nickolsky, World Scientific, Singapore, p.676, (1990).
- [49] I. O. Kulik, Fiz. Nizk. Temp. **17**, 1195, (1991) [Sov. J. Low Temp. Phys. **17**, 628, (1991)].
- [50] I. O. Kulik, Sverhprovodimost': Fiz. Khim. Tekh. (Kurchatov Inst. of Atomic Energy, Moscow) **2**, 175, (1989) [Sov. Superconductivity: Phys. Chem. Tech. **2**, 201, (1989)].

- [51] I. O. Kulik, *Contraction of Atomic Orbitals in the Oxygen Anion Network and Superconductivity in Metal Oxide Compounds*, submitted to Physical Review B, (1994).
- [52] Elliot H. Lieb and F. Y. Wu, *Absence of Mott Transition in An Exact Solution of the Short-Range, One Band Model in One Dimension*, Physical Review Letters **20**, 1445 (1968).
- [53] M. Peshkin, Physical Review A **23**, 360, (1981).
- [54] M. Peshkin and A. Tonomura: *Lecture Notes in Physics, The Aharonov-Bohm Effect*, Springer-Verlag Berlin Heidelberg, (1989).
- [55] J. Robert Schrieffer, *Theory of Superconductivity* (W. A. Benjamin, Elmsford, NY, 1964). Douglas J. Scalapino, in *Superconductivity*, Vol. 1, ed. by R. D. Parks (Marcell Dekker, New York, 1969), p. 449. W. L. McMillan and J. M. Rowell, in *Superconductivity*, Vol.1, ed. by R. D. Rowell (Marcel Dekker, New York, 1969), p. 561.
- [56] D. Yu. Sharvin and Yu. V. Sharvin, *Magnetic flux quantization in a cylindrical film of a normal metal*, JETP Letters **34**, 272, (1981).
- [57] A. Tonomura In: *Lecture Notes in Physics, The Aharonov-Bohm Effect*, Springer-Verlag Berlin Heidelberg, (1989).
- [58] C. N. Yang, Proc. of the International Symposium 'Foundations of Quantum Mechanics', Tokyo, 1983, ed. S. Kamefuchi et al. (Physical Society of Japan, 1984) p. 5.
- [59] A. A. Zvyagin, *Theory of Current States in The Hubbard Chain*, Sov. Phys. Solid State **32**, 905 (1990).
- [60] A. Ferretti, I. O. Kulik, A. Lami, *Flux Quantization and Diamagnetic Currents in Strongly Correlated Systems*, Physical Review B **47**, 12235, (1993).

- [61] Kong-Ju-Bock Lee and P. Schlottmann, *Thermodynamic Bethe-ansatz equations for the Hubbard chain with an attractive interaction*, Physical Review B **38**, 11566, (1988).
- [62] D. J. Scalapino, Physical Review B **44**, 6909, (1991).
- [63] V. Ambegaokar, and U. Eckern, Physical Review Letters **65**, 381, (1990).